Calhoun: The NPS Institutional Archive

DSpace Repository

Theses and Dissertations	1. Thesis and Dissertation Collection, all items

1946

Some studies of expansion rings in rocket motors

Kleiss, Norman J.; Kerkering, Stanley W.; Kleiss, Norman J.; Kerkering, Stanley W.

California Institute of Technology

http://hdl.handle.net/10945/6541

This publication is a work of the U.S. Government as defined in Title 17, United States Code, Section 101. Copyright protection is not available for this work in the United States.

Downloaded from NPS Archive: Calhoun

http://www.nps.edu/library

Calhoun is the Naval Postgraduate School's public access digital repository for research materials and institutional publications created by the NPS community. Calhoun is named for Professor of Mathematics Guy K. Calhoun, NPS's first appointed -- and published -- scholarly author.

Dudley Knox Library / Naval Postgraduate School
411 Dyer Road / 1 University Circle
Monterey, California USA 93943

SOME STUDIES OF EXPANSION RINGS IN ROCKET MOTORS

BY
NORMAN J. KLEISS
STANLEY W. KERKERING

Thesis
K58

Library
U. S. Naval Postgraduate School
Annapolis, Md.

SOME STUDIES OF EXPANSION RINGS IN ROCKET MOTORS

Thesis by

Comdr. N. J. Kleiss, U.S.N.

Lt. Comdr. S. W. Kerkering, U.S.N.

In Partial Fulfillment of the Requirements
for the Professional Degree in Aeronautical Engineering

California Institute of Technology
Pasadena, California

1946

Thesis
K58

ACKNOWLEDGMENT

In presenting this thesis, the authors wish to express their appreciation and gratitude to Dr. E. E. Sechler and Dr. L. G. Dunn of the Guggenheim Aeronautical Laboratory, California Institute of Technology for their supervision, helpful suggestions, and assistance in carrying out the research.

TABLE OF CONTENTS

	SUBJECT	PAGE
	Summary	1
I	Introduction	2
II	Equipment and Test Procedure	4
III	Theoretical Analyses	7
	1. Two Dimensional Bending Analysis	8
	2. Empirical Three Dimensional Membrane Analysis	15
	3. Elastic Three Dimensional Membrane Analysis	19
IV	Discussion of Results	26
V	References	31
VI	Index to Tables	32
VII	Index to Figures	32
VIII	Index to Photographs	32

TABLE OF SYMBOLS

F	Total axial force, lbs/in., at any station defined by r_o. Positive downward.
H	Tensile force, lbs/in., tending to produce axial deformation. (Total H force on one end of specimen = 2 $H(h + 1/2r)$
p	Internal pressure, p.s.i.
r	Small radius of torus, inches. (r = 1" for cases tested.)
R	Large radius of torus, inches. (R = 6.3125" for cases tested.)
r_o	Distance of point from axis of torus.
r_1, r_2	Radii of curvature of a shell in the form of a surface of revolution in meridional plane and in the normal plane perpendicular to meridian, respectively.
N_ϕ, N_θ	Membrane forces per unit length of principal normal sections acting meridionally and perpendicular to the meridian, respectively.
S	$1/2\ S_T$
S_T	Total elongation of expansion joint
ϕ	Angle defined by the intersection of r_2 with axis of revolution. (Three dimensional theory.)
ϕ^1	Value of ϕ after deformation. (Three dimensional theory.)
θ	Angle between perpendicular to axis and perpendicular to shell (Two dimensional theory.)
M	Moment at section mn (two dimensional theory)
t	Thickness of expansion ring
U	Energy (Two dimensional theory)

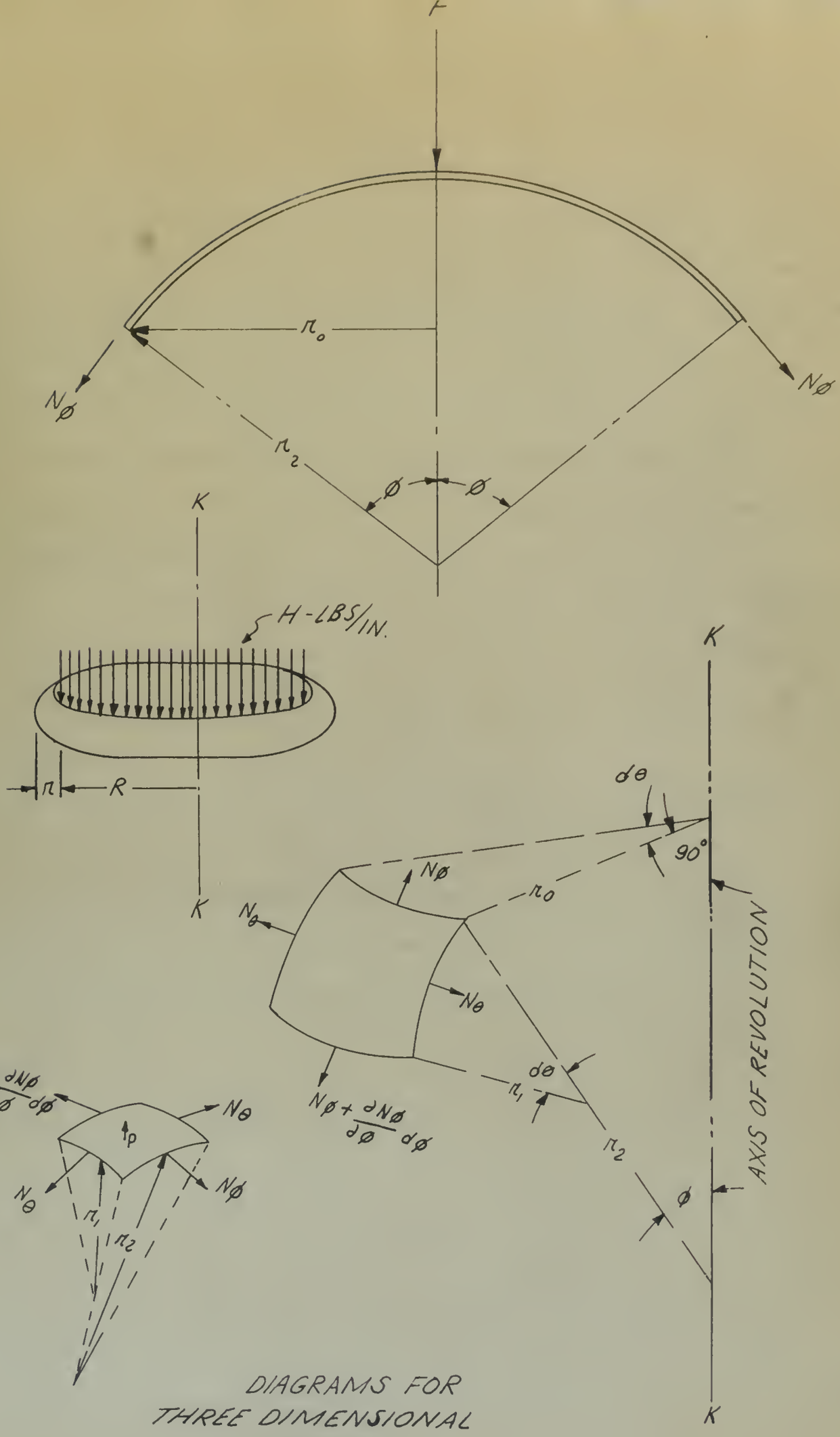

DIAGRAMS FOR THREE DIMENSIONAL THEORIES

SUMMARY

The purpose of this investigation was to investigate the stresses encountered for a semicircular expansion joint for a rocket motor. Information was desired to relate these stresses to the various parameters of the problem.

The stresses involved in this design were found to approximate those indicated by the exact membrane theory. The specimen having the lesser thickness was found to agree more closely with the exact membrane theory, and gave the lowest value of stresses.

An empirical method of membrane analysis, based on deformation profiles, was developed. This method is applicable for stresses slightly above the elastic limit and may be extrapolated for higher values.

The design tested was found to be inherently unsatisfactory on the basis of tests and theoretical considerations.

An alternative design was indicated which would have lower values of stress for a given value of deformation, and which could be designed strictly on the basis of theoretical calculations.

INTRODUCTION.

The increasing interest in rocket motors has focused attention on the lack of data available in connection with the design of safe and efficient expansion joints for the rocket assembly. These expansion joints must withstand high fuel pressures and must allow large degrees of expansion and contraction due to temperature variation. The external radial dimensions of the expansion joint are limited by aerodynamic considerations and the internal dimensions are limited by fuel flow requirements. After fulfilling these physical requirements the design must then be governed by ease of production, assembly, and maintainence.

In an effort to aid in finding the most suitable type, tests were made on two different expansion joint specimens.

Fig. 1 shows in a simplified form the combustion chamber, fuel chamber, and expansion joint of a typical rocket motor. The high temperature due to combustion causes an elongation of the inner chamber, which in turn causes the outer cylinder to elongate. High fuel pressures are present between the outer and inner walls. It is necessary for the expansion joint to withstand the stresses caused by both the elongation and internal fuel pressure. With the assumed temperature distribution as noted in Fig. 1, the elongation in ten inches due to temperature is approximately 0.155 inches.

Information desired from the tests included the relation, at various internal pressures, between elongation of the specimen and the

stresses in the expansion ring, the loading which would give permanent set, and the amount of repeated loadings necessary to cause fatigue failure.

The two specimens tested differed only in the thickness of the expansion joint shell. Time permitted carrying out of only a small part of the desired program.

In addition, three theories were developed: the first, a two-dimensional theory based on bending and energy equations; the second, a three dimensional membrane theory, called the empirical membrane theory, based on the assumption that the expansion ring deforms into an ellipse when elongated; and the third, a general three-dimensional membrane analysis, called the elastic membrane theory. A comparison was made between the rationalized results and the actual test data.

On the basis of these theories the inherent unsatisfactory nature of the expansion rings tested became apparent and a more suitable type was proposed.

EQUIPMENT AND TEST PROCEDURE

An illustration of the test specimen is shown in Fig. 2. The entire assembly was constructed of 1020 steel. The expansion ring and the two end plates were welded in place. On the first specimen the expansion ring had a thickness of 0.05 inches, while on the second specimen the thickness was 0.04 inches. Internal pressure was obtained by the use of a Blackhawk hydraulic jack which forced oil into a 5/8" hole at the top of the specimen. Either two steel bars or two steel plugs were screwed into the center of the top and bottom plates depending whether it was necessary to place the specimen in tension or compression. This tension or compression was accomplished in a Southwark 300,000 lb. testing machine. Control and accuracy allowable by this machine is excellent.

Provision was made for applying a centralized load without bending moments wherever possible. Spherical bearings were used in tension tests, and ball bearing pyramids were used in compression when applied loads were below 40,000 lbs. Beyond this point lead washers were used to centralize the load.

SR-4 strain gages, type A-8, manufactured by the Baldwin Locomotive Works, were used. Five gages were located on the first specimen as illustrated. In order to obtain a better average stress eight gages were used on the second specimen. Their locations are likewise shown.

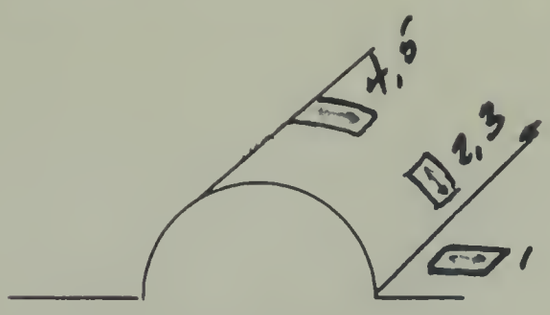

Specimen No. 1

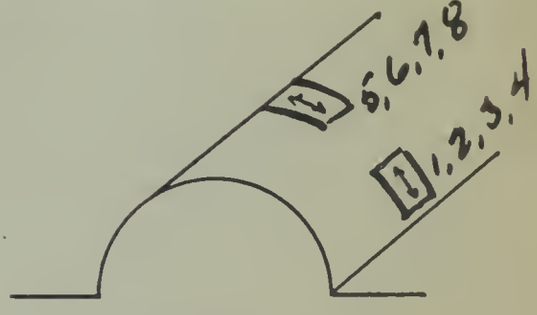

Specimen No. 2

These strain gages were used in conjunction with a multiple channel wheatstone bridge designed and made at the California Institute of Technology. Voltage measurement was made by a Leeds and Northrop Potentiometer. This apparatus was capable of measuring the change in voltage in the strain gages to an accuracy of 0.001 millivolt. It permitted the determination of the change in voltage when the gages were in either tension or compression.

Two gages, located 90° apart, were employed to measure the overall elongation of the specimens. The first was a vernier micrometer which was capable of measuring within 0.001" accuracy; and the second, a dial gage, was capable of measuring within 0.0005" accuracy. The mean of their readings was taken as standard.

Calibrations were first made on the SR-4 strain gages. A gage was glued to each side of a standard 24ST test specimen. The specimen was placed in a testing machine and the strain gage voltages for various tensile forces were recorded as noted in Table I.

Elongations were calculated by the usual theoretical methods and checked by Huggenberger strain gages. From this data the stress-millivolt relation for steel was determined as shown in Table I. This relation is plotted in Fig. 3.

Specimen No. 1 was mounted in the Southward testing machine, as illustrated in Photographs No. I and No. II, and elongated with internal pressures varying from zero to 600 # per sq. in. The voltage across each strain gage was recorded for each combination of pressure and elongation, and the results tabulated in Table II. The stresses as determined from Table II and Fig. 3 are recorded in Table III.

In most instances the specimen had to be placed under compression by the Southwark testing machine in order to prevent the internal pressures from elongating the specimen past the elastic limit.

With an internal pressure of 600 , the specimen was then allowed to elongate until an overall charge in length of 0.2 inches was reached. This was well past the elastic limit of the material. The results are recorded in Tables II and III.

Finally, with a constant pressure of 600 , the elongation was varied between zero and 0.2" until rupture occurred.

The procedure for testing the second specimen was similar to that of the above.

In Figs. 4 through 21 are plotted values from Table III. Two types of graphs were made: one of stress versus elongation with internal pressure as a parameter, and the other of stress versus pressure with elongation as a parameter.

THEORETICAL ANALYSES

Three theoretical approaches were made to the problem and an attempt made to relate the results to the test data.

The first method was a two-dimensional analysis using the energy equation 8. This method assumes that the energy goes into bending and hoop stresses.

The second method involved an empirical three dimensional membrane approach assuming that the pattern of the expansion ring takes the form of an ellipse when elongated. This method is designed to give greatest accuracy for comparatively large elongations and does not necessarily hold too well for small elongations.

The third method was an exact three dimensional membrane approach on the basis of theoretical membrane deflection and stresses. It holds only when all parts of the membrane are within the elastic limit.

The three methods are presented in detail on the following pages.

FIRST METHOD

TWO DIMENSIONAL THEORY

As a first approach in rationalizing the problem, a two dimensional energy analysis was made. This method essentially followed the procedure outlined in Ref. 2, Page 79. It is assumed that the energy is absorbed by bending of the ring and by an increase in the ring diameter caused by "hoop" stresses. It neglects the fact that the specimen is considerably more rigid in the three dimensional case than in the two dimensional case.

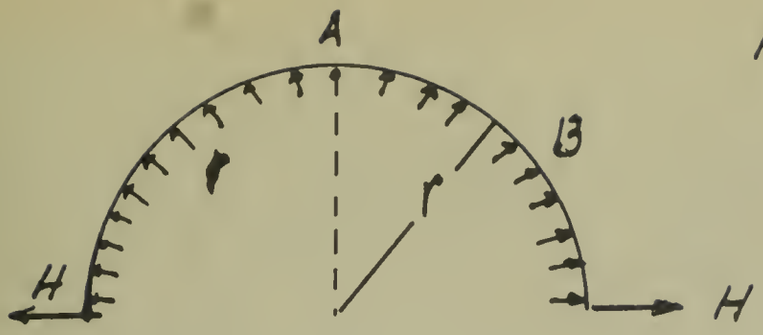

MOMENT AT STATION MN

$$M = M_0 - (H+pr)(r - r\cos\theta) + p r^2\left[\frac{\sin^2\theta}{2} + \frac{(1-\cos\theta)^2}{2}\right]$$

$$= M_0 - Hr + Hr\cos\theta - pr^2 + pr^2\cos\theta + pr^2(1-\cos\theta)$$

$$= M_0 - Hr + Hr\cos\theta$$

$$\frac{dM}{dM_0} = 1$$

$$U = \int_0^S \frac{M^2 ds}{2EI} \qquad \frac{dU}{dM_0} = 0$$

$$0 = \frac{d}{dM_0}\int_0^{\pi/2} \frac{M^2 r\,d\theta}{2EI} = \frac{1}{EI}\int_0^{\pi/2} M\frac{dM}{dM_0} r\,d\theta - \frac{1}{EI}\int_0^{\pi/2} M r\,d\theta$$

$$= \frac{r}{EI}\int_0^{\pi/2}(M_0 - Hr + Hr\cos\theta)\,d\theta$$

$$= \frac{r}{EI}\left[M_0\theta - Hr\theta + Hr\sin\theta\right]_0^{\pi/2}$$

$$= \frac{r}{EI}\left[\frac{M_0\pi}{2} - \frac{Hr\pi}{2} + Hr\right]$$

$$M_0 = Hr - \frac{2Hr}{\pi} = 0.365\,Hr$$

$$M = Hr\cos\theta - 0.635\,Hr = Hr(\cos\theta - 0.635)$$

$$U = \frac{1}{2}\int_0^{\pi/2} \frac{M^2}{EI} r\,d\theta = \frac{H^2 r^3}{2EI}\int_0^{\pi/2} (\cos^2\theta - 1.27\cos\theta + .404)\,d\theta$$

$$= \frac{H^2 r^3}{2EI}\left[\frac{\theta}{2} + \frac{\sin 2\theta}{4} - 1.27\sin\theta + 0.404\theta\right]_0^{\pi/2}$$

$$= \frac{H^2 r^3}{2EI}\left[\frac{\pi}{4} - 1.27 + \frac{0.404\pi}{2}\right]$$

$$= \frac{H^2 r^3}{2EI}(0.150)$$

$$\frac{dU}{dH} = \delta_1 = 0.150\frac{Hr^3}{EI}$$

The contribution of p to the deflection:

Circumferential stress $= \sigma = \frac{pd}{2t}$

Elongation $= e = \frac{\sigma}{E}L = \frac{pd}{2tE}\pi d$ (of circumference)

The change in diameter $= \delta_2 = \frac{e}{\pi} = \frac{2pr^2}{tE}$

Total Elongation:

$$\delta_T = 2\delta_1 + \delta_2 = 2\times 0.15\frac{Hr^3}{EI} + \frac{2pr^2}{tE}$$

$$= 0.30\frac{Hr^3}{EI} + \frac{2pr^2}{tE}$$

$E = 30 \times 10^6$ for steel

$I = \frac{t^3}{12}$

$$\delta_T = \frac{0.30 H r^3}{30 \times 10^6 \frac{t^3}{12}} + \frac{2}{30 \times 10^6} \times \frac{\phi r^2}{t}$$

$$= 1.2 \times 10^{-7} \frac{H r^3}{t^3} + 0.667 \times 10^{-7} \frac{\phi r^2}{t} \qquad (1)$$

For Point "A"

$$\sigma_A = \frac{H + \phi r}{t} - \frac{M_0 y}{I}$$

$M_0 = .365 H r$

$y = t/2$

$I = \frac{t^3}{12}$

$$\sigma_A = \frac{H + \phi r}{2} - 6\left(\frac{.365 H r}{t^2}\right) \qquad (2)$$

For First Specimen: $t = .05''$; $r = 1''$

$$\sigma_A = 20H + 20\phi - 876H \text{ ; or } H = \frac{20\phi - \sigma_A}{856} \qquad (3)$$

and $$\delta_T = 1.2 \times 10^{-7} \frac{H}{(.05)^3} + 0.667 \times 10^{-7} \frac{\phi}{.05}$$

$$= 0.96 \times 10^{-3} H + 13.34 \times 10^{-7} \phi$$

Subst (3)

$$\delta_T = 0.96 \times 10^{-3}\left(\frac{20\phi - \sigma_A}{856}\right) + .1334 \times 10^{-5} \phi$$

$$\sigma_A = 20.2\phi - 894000\delta_T$$

FOR SECOND SPECIMEN: $t = .04''$, $r = 1''$

$$\sigma_A = 25H + 25\phi - 1370H$$

$$H = \frac{25\phi - \sigma_A}{1345}$$

$$\delta_T = 1.2 \times 10^{-7} \frac{H}{(.04)^3} + 0.667 \times 10^{-7} \frac{\phi}{.04}$$

$$= 1.2 \times 10^{-7} \left[\frac{25\phi - \sigma_A}{1345\,(.04)^3} \right] + 16.675 \times 10^{-7} \phi$$

$$= -13.92 \times 10^{-7} \sigma_A + 364.67 \times 10^{-7} \phi$$

$$\sigma_A = 26.2\,\phi - 718000\,\delta_T$$

POINT "B": WHERE $\theta = 57.3°$

$$M = HM(\cos\theta - 0.635)$$

$$= -.095\,HM$$

FOR 1ST SPECIMEN: $t = .05''$; $r = 1''$

$$\sigma_B = \frac{\phi d}{2t} + \frac{H\cos\theta}{t} - \frac{M y}{I}$$

$$= \frac{\phi + 0.541H}{t} + \frac{.095H \times 1/2}{t^3} \cdot \frac{t}{2}$$

$$= 20\phi + 10.8H + 228H$$

$$H = \frac{\sigma_B - 20\phi}{238.8}$$

$$\delta_T = 0.96 \times 10^{-3} H + 13.34 \times 10^{-7} p$$

$$= 0.96 \times 10^{-3} \left[\frac{\sigma_B - 20p}{238.8} \right] + 13.34 \times 10^{-7} p$$

$$= .402 \times 10^{-5} \sigma_B - 8.05 \times 10^{-5} p + 13.34 \times 10^{-7} p$$

$$= .402 \times 10^{-5} \sigma_B - 7.917 \times 10^{-5} p$$

$$\sigma_B = 249000\, \delta_T + 19.7\, p$$

2nd SPECIMEN: $t = .04''$, $r = 1''$

$$\sigma_B = \frac{p + 0.541 H}{t} + \frac{.095 H \times 6}{t^2}$$

$$= 25p + 13.5H + 356H$$

$$H = \frac{\sigma_B - 25p}{369.5}$$

$$\delta_T = \frac{1.2 \times 10^{-7}}{(.04)^3} H + 0.667 \times 10^{-7} \frac{p}{.04}$$

$$= \frac{1.2}{640} H + 16.675 \times 10^{-7} p$$

$$= \frac{1.2}{640} \left[\frac{\sigma_B - 25p}{369.5} \right] + 16.675 \times 10^{-7} p$$

$$= 5.07 \times 10^{-6} \sigma_B - 12.7 \times 10^{-5} p + 16.675 \times 10^{-7} p$$

$$\sigma_B = 197000\, \delta_T + 24.7\, p$$

SUMMARY of TWO DIMENSIONAL THEORETICAL EQUATIONS

FIRST SPECIMEN: ($t = .05''$)

$$\sigma_A = 20.2\beta - 894000\,\delta_T$$

$$\sigma_B = 249000\,\delta_T + 19.7\beta$$

SECOND SPECIMEN: ($t = .04''$)

$$\sigma_A = 26.2\beta - 718000\,\delta_T$$

$$\sigma_B = 197000\,\delta_T + 24.7\beta$$

THESE VALUES ARE PLOTTED IN FIGURES 22, 23, 24 and 25 and COMPARED WITH the ACTUAL TEST VALUES IT IS NOTED that the AGREEMENT IS NOT GOOD FOR POINT A and is ONLY APPROXIMATE AT POINT B.

[illegible] METHOD

[illegible] THREE DIMENSIONAL [illegible] ANALYSIS

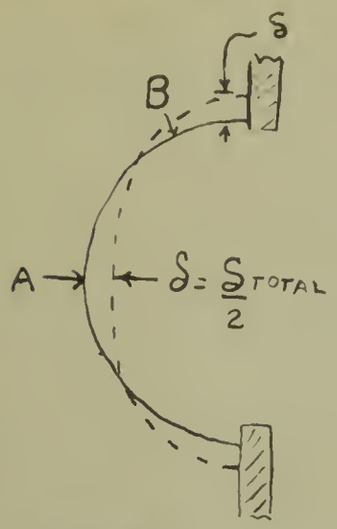

Fig. a

This theory assumes that bending stresses are small in relation to membrane stresses and that bending produces only local effects. Membrane stresses are computed for the initial condition and for the observed deformation pattern at comparatively large values of elongation (i.e., in the vicinity of the elastic limit), thereby providing a basis of empirical design if test data is compatible with membrane theory.

The observed deformation curve was found to resemble an ellipse with the minor axis shortened 0.035" and the major axis lengthened 0.035" for stresses slightly above the elastic region. Near the weld, the ellipse was observed to be slightly distorted at large values of elongation.

This method assumes elliptical distortion in the manner noted above and derives equations which give stresses corresponding to this distortion in terms of the various parameters. Essentially, this procedure is a variation of the method given in Art. 73 of Ref. 1.

FOR THE POINT A (See Fig. a)

$$2\, r_o N_\phi \sin\phi + F = 0$$

But $-F = \pi p(\overline{\quad} + r - \delta^2 - 1^2) + N(1 + 1/2r)\, 2\pi$

Substituting: $(\phi = 90^\circ)$

$2r_o N\phi - p(r^2 + 2rR - 2Rr - rR) - 2H (R + 1/2r) = 0$

but $r_o = R + r - S$

$$N_\phi = \frac{p(r^2 + 2rR - 2Rr - Rr) + 2H (R + 1/2r)}{(2) (R + r - S)}$$

(1) $$\sigma_n = \frac{1}{t} \quad \frac{p(r^2 + 2rR - 2Rr - Rr) + 2H (R + 1/2r)}{(2) (R + r - S)}$$

for the case tested, $N_\phi = 0.933p (1 - 0.95S_p) + 0.933H$

$$N_\theta = r_2 \left(p - \frac{N\phi}{r_1}\right)$$

From the deformation pattern we know that the band at center contracts a distance of 2δ if p = const. This corresponds to a N_θ stress of value

$$\sigma_2 = \epsilon E = \frac{\delta}{(R + r)} \quad E$$

for the cases tested σ_2 = 4,100,000# (within elastic limit)

This induces a tensile stress in the meridional direction N_ϕ equal to:

(2) $$\sigma_1 = \nu\epsilon E = \frac{\delta E}{R + r}$$

σ_1 for the cases tested = 1,230,000 #

The above correction does not include the effect of the original stress due to N_θ. This stress is a compressive stress of value

(3) $$\sigma_3 = - \nu \frac{p}{t} (r - \delta)$$

σ_3 for the cases tested = $- 0.3 \frac{p}{t} (1 - \delta)$

The total meridional stress at "A" is the sum of equations (1), (2), and (3).

For the cases tested

$$\sigma_1 = \frac{1}{t}\left[0.634p + 0.914H\right] + 615{,}00\,\delta_2 - 0.15\,\frac{p}{t}\,\delta_T$$

For a second point B, located at $\beta = 60^\circ$, the following equations were derived.

$$r_1 = \frac{\left[r - \frac{1}{4}\frac{\epsilon}{r} + \left(\frac{\epsilon}{r}\right)^2\right]^{3/2}}{r - \left(\frac{\epsilon}{r}\right)^2}$$

$$\tan \phi = .5831\ \frac{r + \frac{\epsilon}{r}}{r - \frac{\epsilon}{r}}$$

By graphic construction

$$r_2 = 15.08\ r_1$$

The equation

$$\frac{n_\phi}{r_1} + \frac{n_\theta \sin \phi}{15.08 r_1} = p$$

can now be solved by assuming a value of $n_\theta = p$ from equilibrium considerations. This gives the following stress at B due to direct membrane stress.

$$(4)\quad \sigma = \frac{p}{t}\left\{ \frac{\left[r - .25\frac{\delta}{r} + \left(\frac{\delta}{r}\right)^2\right]^{3/2}}{r - \left(\frac{\delta}{r}\right)^2} - 0.0469p \right\} + \frac{+0.500H}{t}$$

It should be noted that the above equation holds only for a given value of the r/t ratio having the proportion 1 : 7.3215. (Calculations became too complex to retain this parameter.)

In computing the above meridional stress the value of N_θ was assumed to be of magnitude p. The correction to the above meridional stress to allow for this is

(5) $$\sigma_1 = -\nu \frac{p}{t}$$

Mechanical construction further indicates that the point B suffers 1/4 the radial compression in comparison to the compression at point A. The stress corresponding to the compression of the radial band at A has the value

(6) $$\sigma_2 = 1/4 \quad \frac{E \Delta}{L}$$

The total meridional stress at point B is the sum of equations (4), (5), and (6).

The plots of σ_T vs. δ_T for points A and B are given in Fig. 28 to 31, showing computed and experimental values.

It should be noted that the stress curve for point B will tend to become negative at large values of deformations due to the local bending in the region of the weld. For this reason the stress curves for point B are not continued for a value of δ_T exceeding 0.070".

These stresses apply at relatively large deformations since the stresses fit the actual deformation pattern at large deformations. They do not apply for small deformations.

THIRD METHOD
ELASTIC THEORY DIFFERENTIAL EQUATIONS

This theory applies where deflections are large in relation to thickness and all stresses are within the elastic limit. This method is based on Art. 73 and 76 of Ref. 1.

(1) $\frac{N_\phi}{r_1} + \frac{N_\theta}{r_2} = p$

(2) $2\pi r_o N_\phi \sin\phi + F = 0$ where F is total downward force at any station defined by r_o

These two equations define all forces acting on a unit element.

Solving (2) for N_ϕ gives

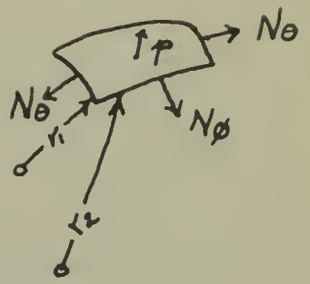

(3) $N_\phi = -\frac{F}{2\pi r_o \sin\phi}$

Eliminating N_ϕ from (1) gives

(4) $N_\theta = r_2 p + \frac{r_2}{r_1}\left(\frac{F}{2\pi r_o \sin\phi}\right)$

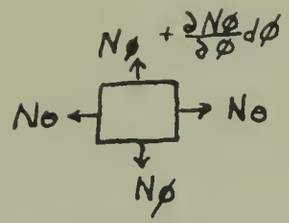

Fig. b.

Fig. a.

Total force measured in meridional direction by strain gage is

(5) $F_T = N_\phi - \nu N_\theta$

(6) $F_T = -\nu r_2 p - \nu\frac{r_2}{r_1}\left(\frac{F}{2\pi r_o \sin\phi}\right) - \frac{F}{2\pi r_o \sin\phi}$

$$F_T = -\left[\left(\frac{F}{2\pi r_o \sin\phi}\right)\left(1 + \nu\frac{r_2}{r_1}\right) + \nu r_2 p\right]$$

(7) $\sigma_T = -\frac{1}{t}\left[\frac{F}{2\pi r_o \sin\phi}\left(1 + \nu\frac{r_2}{r_1}\right) + \nu r_2 p\right]$

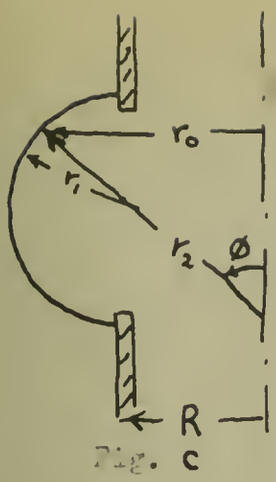

Fig. c

$$P = \left\{\begin{matrix}\text{total downward load} \\ \text{at station } r_o\end{matrix}\right\} = -42H - \pi(r_o^2 - R^2)\,p$$

$$r_o^2 = \overline{R + r_1 \sin\phi}^2 = R^2 + 2Rr_1 \sin\phi + r_1^2 \sin^2\phi$$

$$P = 42H - \pi(2Rr_1 \sin\phi + r_1^2 \sin^2\phi)p$$

Equation (7) then becomes

$$(8)\quad \sigma_T = -\frac{1}{t}\left[\left(\frac{-42H - \pi(2Rr_1 \sin\phi + r_1^2 \sin^2\phi)p}{2\pi r_o \sin\phi}\right)\left(1 + \nu\frac{r_1}{r_2}\right) + \nu r_2 p\right]$$

By definition $r_o = r_2 \sin\phi = R + r_1 \sin\phi$

$$(9)\quad \sigma_T = -\frac{1}{t}\left[\left(-\frac{42H}{2\pi \sin\phi\,(R + r_1 \sin\phi)} - p\,\frac{2Rr_1 + r_1 \sin\phi}{2R + 2r_1 \sin\phi}\right)\left(1 + \nu\frac{r_2}{r_1}\right) + \nu r_2 p\right]$$

Equation (9) permits determination of the best ratios for the parameters r and R in regard to meridional stress at any point.

We will make a study of the condition where

$r = 1"$

$R = 6.3125"$

$r_1 \approx r$

$$(9)'\quad \sigma_T = \frac{1}{t}\left[\left(\frac{6.8125\,H}{\sin\phi(6.3125 + \sin\phi)} - \frac{p(12.625 + \sin\phi)}{12.625 + 2\sin\phi}\right)\left[1 + \nu\left(\frac{R}{\sin\phi} + 1\right)\right] + \nu p\left(\frac{R}{\sin\phi} + 1\right)\right]$$

Consider stress at point A: ($\phi = 90^\circ$)

$$\sigma_T = -\frac{1}{t}\left[(-0.933H - 0.933\,p)\left[1 + \nu(7.3125)\right] + \nu p(7.3125)\right]$$

assume $\nu = 0.3$

$$(10)\quad \sigma_T = \frac{1}{t}\left[2.98H + 0.7863p\right]$$

For the two cases tested, stresses at "A" have values:

σ_T (for t = 0.04) = 72H + 19.68p

σ_T (for t = 0.05) = 59.6H + 15.726p

At point B: ($\phi = 32.7^\circ$)

Substituting in (9)' Sin ϕ = 0.54

$$\sigma_T = -\frac{1}{t}\left[\left(-\frac{6.8125H}{3.75} - \frac{13.156p}{13.706}\right)\left(1 + J(12.7)\right) + J(12.7)p\right]$$

$$(11)\quad \sigma_T = \frac{1}{t}\left[8.725H + 0.795p\right]$$

for the two cases tested, stresses at point "B" have values:

σ_T (for t = 0.04") = 218 H + 19.9p

σ_T (for t = 0.05") = 174.5 H + 15.9p

The deflection curve may now be computed by the method of Art. 76 of Ref. 1.

A study of the equation

$$V = \text{Meridional elongation} = \sin\phi \cdot \left\{\int \frac{f(\phi)}{\sin\phi}\, d\phi + C\right\}$$

readily shows that V gets very large at small values of ϕ since $f(\phi)$ is a function of $\left(\frac{1}{\sin(\phi)} + \frac{2}{\sin^2\phi}\right)$

The radial elongation acts in a similar manner.

An actual calculation of V showed that the membrane stress is far above the elastic limit for S_T = 0.023" at $\phi = 5^\circ$.

EXTENSION OF ELASTIC MEMBRANE THEORY

From the above considerations in regard to the stresses in the membrane in the vicinity of the weld (bending moment assumed to be

zero) it is readily seen that the elastic membrane theory does not apply for δ_y 0.028" since the membrane stresses have exceeded the elastic limit in the region of the weld.

The elastic membrane theory relates the deformations with stresses. These stresses in turn are a function of radius of curvature at the given point. Conversely, if we know the radius of curvature (and all parts of the membrane are in the elastic region) the stress is determined.

If we can relate the non-elastic radius of curvature to the elastic radius of curvature and substitute this factor in equation (9) we can obtain an idea of the trend in the non-elastic region. This equation is repeated below.

$$(9)\ \sigma_t = \frac{1}{t}\left[\left(\frac{-42\ H}{2\pi \sin\phi\ (R + r_1 \sin\phi)} - p\,\frac{(2Rr_1 + r_1 \sin\phi)}{2R + 2r_1 \sin\phi}\right)\left(1 + \sqrt{\frac{r_2}{r_1}}\right) + \sqrt{r_2 p}\right]$$

Now R is a constant, r_1 is very nearly unity and varies only slightly with large deformations. It will be seen, therefore, that the quantity

$$\left(\frac{-42\ H}{2\pi \sin\phi\ (R + r_1 \sin\phi)} - p\,\frac{(2Rr_1 + r_1 \sin\phi)}{2R + 2r_1 \sin\phi}\right)$$

where $R = 6.3125"$ and $r_1 = 1 \pm 0.1$ (say)
is constant for a given value of ϕ for all practical purposes. The major variables in equation (9) are the terms

$$\left(1 + \sqrt{\frac{r_2}{r_1}}\right) \text{ and } \left(\sqrt{r_2 p}\right)$$

It is apparent from consideration of these two terms that a smaller value of $\frac{r_2}{r_1}$ will give a lower value for σ_T. Non-elastic deformation does just this. The slope of the tangent (in the region of the weld) increases, thereby reducing the radius of curvature and lowering the stress. (See Fig. d.) At point A the effect is negligible. At point B the effect is considerable since the ratio $\frac{r_2}{r_1}$ may change by a factor of eight or nine (based on mechanical construction with $\delta_T = 0.10"$). This means that the stress at B will be lowered by a factor of approximately 3 for such local deformations. (This result is obtained from equation (9).)

The basis of the inflection point at B (See Fig. d.) comes from a study of the radial rigidity of the membrane.

The rigidity, as previously indicated, is a function of $\frac{1}{\sin \phi} + \frac{1}{\sin^2 \phi}$. Since $\sin \phi$ is very small near the weld and the stresses are beyond the elastic limit, the radial resistance to deformation is very slight between point B and the weld. Between point B and point A the radial rigidity increases rapidly and the stresses are below the elastic limit. This makes possible the appearance of an inflection point, or at the very least a discontinuity in the radius of curvature.

EFFECT OF LOCAL BENDING

It should now be noted that local bending stresses at "B" will further decrease the stress at "B". From the change in curvature the bending stress at "B" may be greater than the membrane stress

when deformation becomes large at "B" as shown in Fig. c. This local bending produces a compressive stress. The measured stress at "B" may become very small or negative. A clue to the state where σ_T at "B" may become negative is where the H vs. σ_T curve becomes non-linear. This is at $\delta_T > 0.028"$ where slight discontinuities were encountered for all pressures. It is certain that the preceding equations for stresses at "B" do not apply for $\frac{\delta_I}{\sigma_T} > 0.028"$ as they would indicate too large a stress at "B" (as measured by a strain gage.)

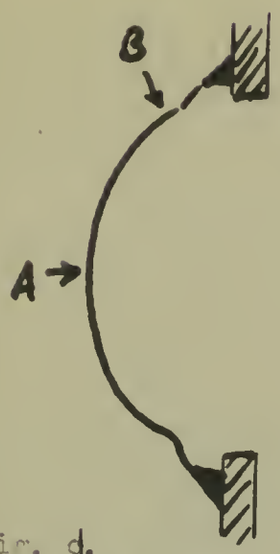

Fig. d.
Deformation Pattern at very large deformations

At point "A" this bending effect is negligible since this region has the least bending. (The effect, however, would be a compressive stress.)

From considerations of the membrane stresses produced near the weld, it is clearly seen that the ratio $\frac{r_2}{r_1} \longrightarrow \infty$ for a small weld and that the membrane stresses become very large until relieved by deformation. At the weld the bending stresses are also tensile stresses at a point infinitely close to the weld. For elongations of the order $\delta_T = 0.20"$ this analysis shows that the type of expansion joint tested is inherently unsatisfactory since stresses cannot possibly be kept below the elastic limit.

In order to further understand the unsatisfactory nature of the original design, the schematic stress distribution at various points (due to both bending and membrane stresses) are shown for a large and a small θ_p. (See Fig. d)

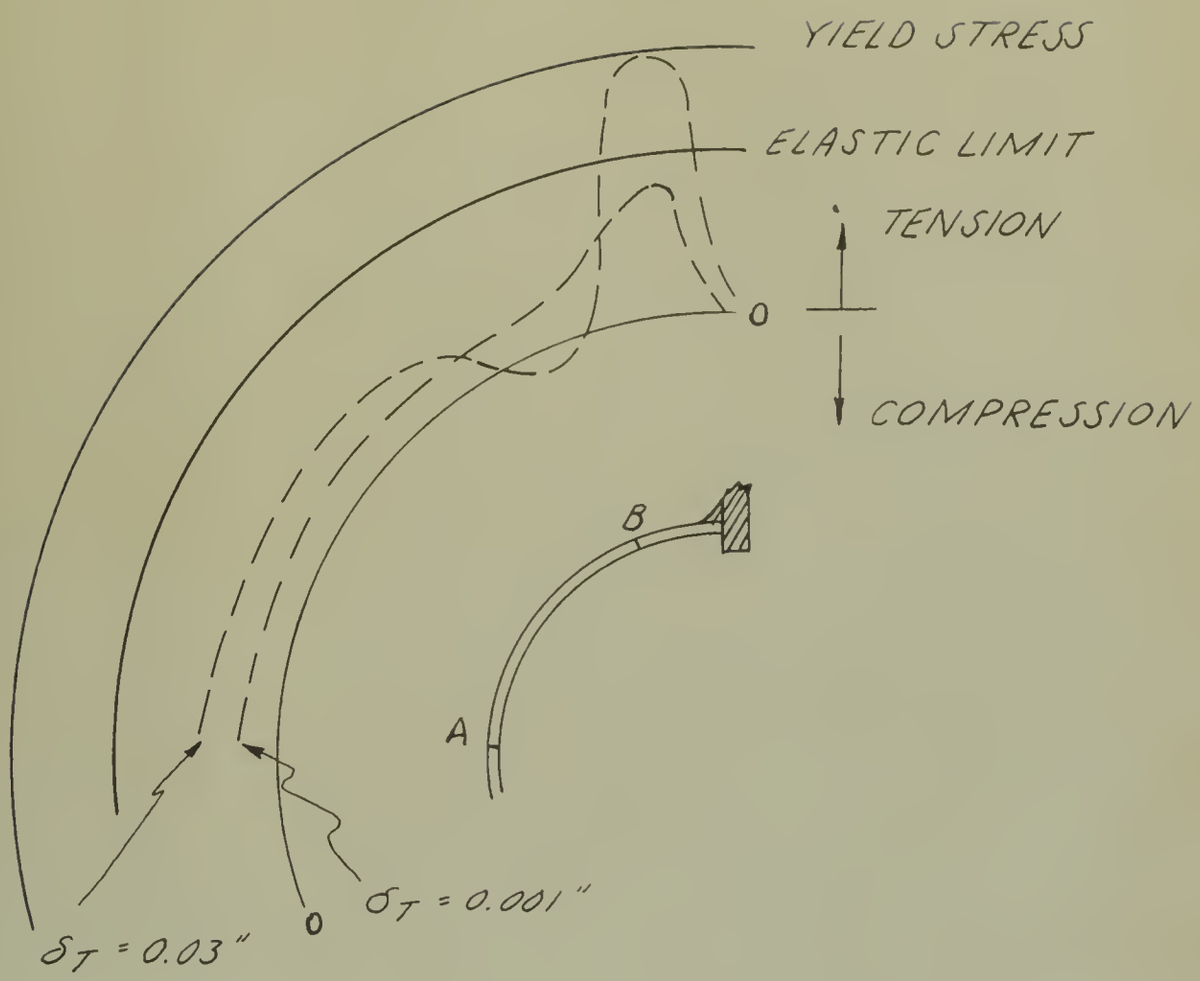
YIELD STRESS
ELASTIC LIMIT
TENSION
0
COMPRESSION
B
A
$\delta_T = 0.001''$
0
$\delta_T = 0.03''$

FIG. α_1

DISCUSSION OF RESULT

By comparison of the calculations for the two dimensional bending theory and observed data, this method was found to be totally inapplicable. The stress distribution, according to this theory, would yield ~~by~~ compressive stresses in the region of point A (the maximum diameter of the expansion joint). Actually, these stresses are tensile stresses and have large magnitudes. Moreover, the stresses at point B should increase with elongation. Actually, they reach a peak, diminish to practically zero, then increase slightly.

The elastic three dimensional membrane theory gives very good agreement, within the limits of experimental accuracy, to the elastic limit. Beyond this point the agreement was unsatisfactory since these equations do not consider the reduced modulus of elasticity. It will be noted that the specimen having the smaller thickness gave better agreement and, incidently, gave lower values of stresses for a given elongation. This validates the applicability of the membrane theory. This theory is further justified by Ref. 1, 3, and 4. The applicability is particularly shown by Art. 67, and 68 of Ref. 1. It should be noted that this theory does not apply when any portion of the membrane exceeds the elastic limit and that this theory has been extended in this thesis to show the qualitative effect of non-elastic deformation. This difficulty comes from the fact that stresses in the original design exceed the elastic limit for infinitesimal deformations.

The empirical three dimensional membrane theory evaluates the membrane stresses for the measured deformations. Since the deformation pattern chosen was one for total elongation equal to 0.035", the agreement is better for large values than for small ones. This method is only as accurate as the measured deformation pattern. Considering this limitation, this method gave remarkably good agreement for values of total elongation equal to 0.200". As noted previously, neither test or computed values were corrected for reduced modulus. This empirical method should be employed only as a last resort where stresses cannot be computed on a strict theoretical basis.

On the basis of these tests and theoretical calculations the type of expansion joint tested was found to be inherently unsatisfactory for the following reasons:

1. This expansion joint experiences permanent deformation for very small elongations. These deformations become appreciable for a total elongation of 0.025", which is far below the requirement of 0.200".

2. The membrane and bending stresses are greatest in the vicinity of the weld. Since the weld material has the weakest physical properties, this is undesirable.

3. The present design is theoretically not sound, and is, therefore, difficult of solution. With a slight modification in design, the expansion joint could be subjected to an exact analysis with ease, and the stresses greatly reduced.

4. The specimen having the greater thickness failed at the weld for one cycle of elongation (from zero to 0.200" elongation and back

to zero at 600 # pressure). The specimen having the lesser thickness failed after experiencing approximately two and one-half such cycles, the failure occurring at three places at the weld.

A suggested expansion joint profile is shown in Fig. e. The proportion r_1, r_a, r_b, R, may be determined analytically by means of Art. 76 of Ref. 1. The procedure would be to choose the average δ_T and p anticipated and solve for "Y" = zero at station Y. This means that the membrane will not deflect outward or inward at this point. Such a calculation would be very tedious but possible. An alternate solution would be to make several specimens and mount them in a manner similar to the method used in this test. Apply internal pressure by a suitable hydraulic pump, control elongation (δ_T) by a screw device, and note the change in a dial gage mounted at station Z. The specimen giving the least change in the dial reading at Z over the required range of p and δ_T would be the best specimen. Bending stresses would be reduced to a minimum and the membrane theory would give great accuracy. Note that the design calls for a positive slope at all points. This avoids infinite values of $\frac{r_2}{r_1}$ or indeterminate stresses. (Theoretical analysis becomes very complex if slope at any point is zero.) Preliminary studies show that a slope of 0.5 is desirable for the minimum value of the slope.

It may, perhaps, be argued that the expansion joint designed in Fig. e is similar to a sylphon and is governed primarily by bending stresses. That is true to a point, but it is only because membrane stresses have been kept in the elastic region. Moreover the bending

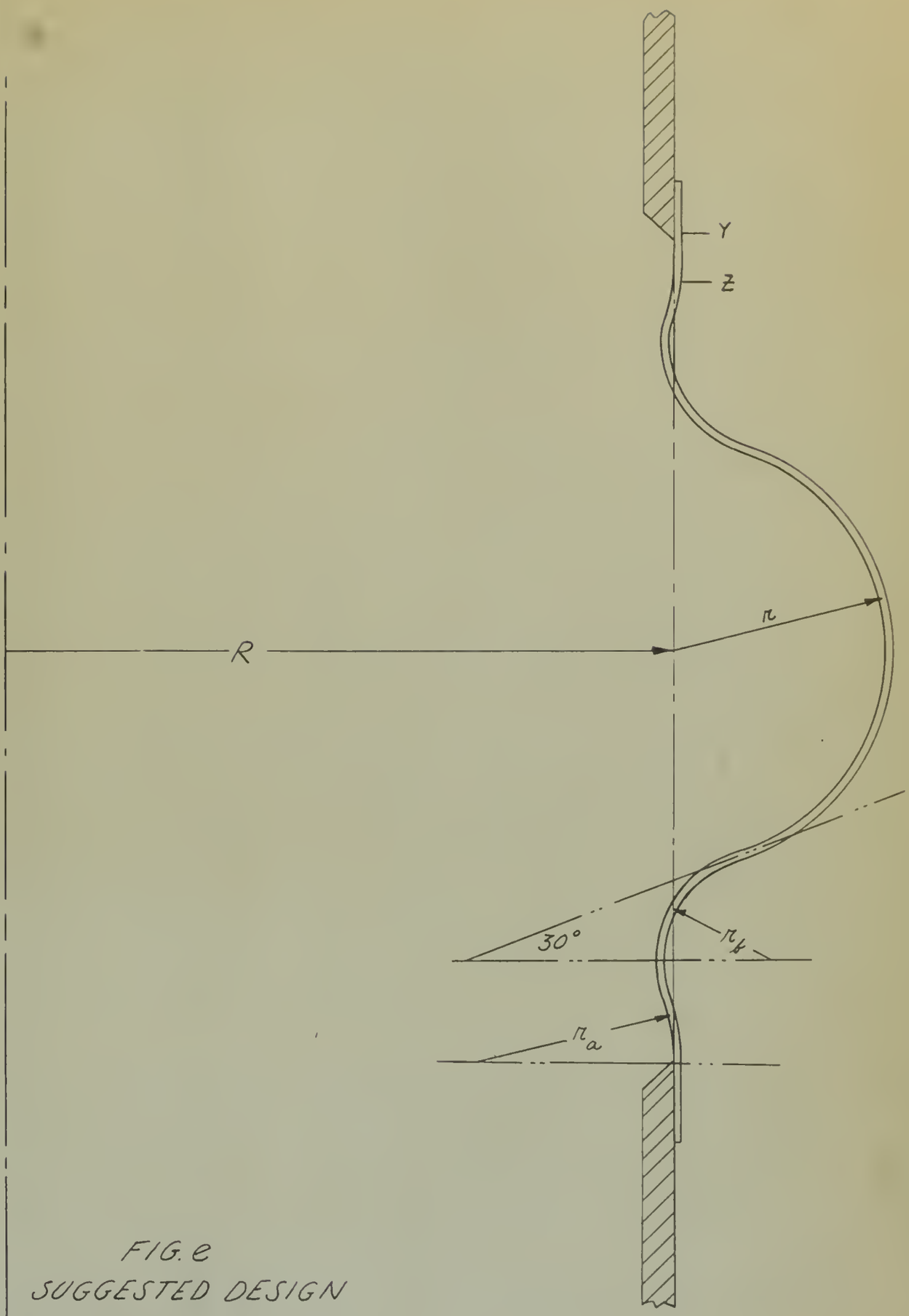

FIG. e
SUGGESTED DESIGN
FOR EXPANSION JOINT

stresses may then be retained in the elastic region. (Note that the bending theory gives stresses above the elastic limit for the point near the weld in original design for $\delta_I = 0.20"$).

It is not stated that the proposed design will give all stresses below the elastic limit. To obtain such a condition it may be necessary to resort to several bands. However, the design offered should have greater resistance to fatigue and may be satisfactory if the number of cycles required is not too great.

In regard to the parameter t (thickness) the theoretical analysis shows that the membrane stresses are inversely proportional to the thickness. This would indicate at first hand that a large value of t is desirable. Theory and the tests show, however, that large values of t set up large bending stresses for a given displacement in bending. This shows that there is an optimum value of t, probably only slightly above that required to keep the stresses in the elastic region.

The remaining parameters, r and R, are more or less determined by rocket design.

ANALYSIS OF TEST RESULTS

Both test and theory agree that stress is determined by the magnitude of H, representing the force per unit length required to produce elongation of the expansion ring. With a low value of H, the stresses will be reduced to a reasonable magnitude.

The additional stress due to internal pressure was found to be practically constant over deformations in the elastic region.

Experimental results in contrast to theoretical values are shown in Figs. 28 to 31. It will be noted that for the first specimen (t = 0.05") a large spread of stresses is obtained for various pressures. For the second specimen (t = 0.04") this variation with pressure was not clearly defined because fewer test points were obtained. In this regard, it is very difficult to obtain accurate readings for small elongations when the specimen has many dents and dimples, as did the specimens tested. At larger elongations these local irregularities tend to be removed by the increased stresses.

It should be noted that the above difficulty would not be encountered with a properly designed and carefully manufactured specimen.

It is believed that the stress readings were obtained with a degree of accuracy consistent with the precision of the specimen but inherent inaccuracies are still sufficient to account for any differences between observed results and the exact membrane theory. It should be noted from Figs. 28 to 31 that the stress variation agrees with theory in respect to elongation, pressure, and location of station; and that the specimen of lesser thickness gives the slightly better agreement and has lower values of stresses than the thicker specimen.

The empirical method, based on radial displacements, was found to be applicable and gave surprisingly good results considering the crudeness of the deformation pattern. The deformation pattern should, of course, be obtained by measuring the radial displacements of numerous stations.

[illegible]

1. Theory of Plates and Shells - S. Timoshenko

2. Strength of Materials, Vol. II - S. Timoshenko

3. Theory of Elastic Stability - S. Timoshenko

4. Theory of Elasticity - S. Timoshenko

INDEX TO TABLES

TABLE I	Strain Gage Calibration
TABLE II	Observed Test Data: Pressure, Elongation and Strain Gage Readings
TABLE III	Observed Stresses

INDEX TO FIGURES

FIGURE 1	Rocket Section
FIGURE 2	Test Specimen
FIGURE 3	Stress - Millivolt Relation for steel
FIGURES 4 thru 21	Observed Stress, Elongation and Pressure Curves
FIGURES 22 thru 25	Two Dimensional Theoretical Curves Versus Test Curves
FIGURES 26 and 27	Curves of R versus S_T
FIGURES 28 thru 31	Three Dimensional Theoretical Curves versus Test Curves

INDEX TO PHOTOGRAPHS

PHOTOGRAPH 1	General View of Test
PHOTOGRAPH 2	Test Specimen

STRAIN GAUGE CALIBRATION

STANDARD SPECIMEN – 2.14 ST

$t = 0.0775$ = THICKNESS (IN)

$W = 0.5$ = WIDTH (IN)

$A = tW = 0.03875$ □" = CROSS SECTIONAL AREA (□")

$E = 10^7$

$\varepsilon = \frac{P}{AE} = \frac{P}{.03875} \times 10^{-7} = 25.8P \times 10^{-7} = 2.58P \times 10^{-6}$

P	$\varepsilon \times 10^{-6}$	GAGE 1	GAGE 2	ΔP	$\Delta \varepsilon$	ΔG_1	ΔG_2
LBS	IN/IN	MV	MV	LBS	$\times 10^{-4}$ IN/IN	MV	MV
150	3.87	.278	.341	50	1.29	.278	.341
200	5.16	.578	.655	50	1.29	.300	.314
250	6.45	.878	.962	50	1.29	.300	.307
300	7.73	1.179	1.21	50	1.28	.301	.304
350	9.03	1.484	1.62	50	1.30	.310	.352
400	10.32	1.784	1.813	50	1.29	.301	.253
450	11.60	2.102	2.112	50	1.28	.318	.199
500	12.90	2.412	2.473	50	1.30	.310	.361
600	15.48	3.022	3.064	50	2.58	.610	.591
700	18.06	3.637	3.668	100	2.58	.617	.604
800	20.64	4.244	4.248	100	2.59	.605	.580
900	23.25	4.863	4.865	100	2.60	.619	.617
1000	25.80	5.465	5.473	100	2.55	.602	.608
1100	28.40	6.063	6.078	100	2.60	.598	.605
			$\Sigma =$		25.82	3.961	3.846

FOR AVERAGE $\Delta P = 50^{\#}$ | 1.291 | .305 | .296

.296

2 | .601

.300

$1\ MV = \frac{1.291 \times 10^{-4}}{0.3}$ IN/IN

FOR STEEL: $1\ MV = \frac{1.291 \times 10^{-4}}{0.3} \times 30 \times 10^6 = 12830$ PSI $= \sigma$

TABLE I

SPECIMEN NO 1

LOAD	P	δ_T	GAGE READINGS - MILLIVOLTS				
lbs	PSI	ELONG. $\times 10^{-3}$	1	2	3	4	5
200	0	2.5	.022	.092	0.110	.067	No
800		5.5	.034	.213	0.258	.099	READING
1400		12.5	.048	.339	.394	.130	1
2000		15	.054	.444	.533	.153	REPLACE
3200		16.5	.057	.765	.879	.212	
4400		21.5	.073	1.017	1.040	.242	
5600		24.0	.084	1.250	1.291	.433	
6800		31.5	.101	1.467	1.53	.823	
8000		33.5	.11	1.761	1.745	1.128	
450	25	19	.064	1.286	1.218	.484	.509
900		16	.068	1.248	1.115	.460	.492
1200		16	.070	1.178	1.074	.437	.476
1500		15	.061	1.173	1.038	.427	.462
1800		13	.071	1.108	0.995	.406	.440
2100		14	.071	1.057	0.975	.381	.421
3700		12	.069	.937	0.81	.350	.403
3300		9	.061	.846	0.672	.184	.375
450	50	23	.112	1.845	1.83	.690	.719
900		22	.09	1.65	1.727	.658	.658
1500		20	.092	1.624	1.547	.603	.632
1800		19	.092	1.60	1.511	.600	.625
2100		18	.091	1.523	1.428	.566	.601
2400		17.5	.100	1.501	1.398	.561	.593
3000		17	.102	1.438	1.293	.527	.570
3600		15	.097	1.346	1.187	.493	.532
4200		13.5	.095	1.25	1.09	.457	.521

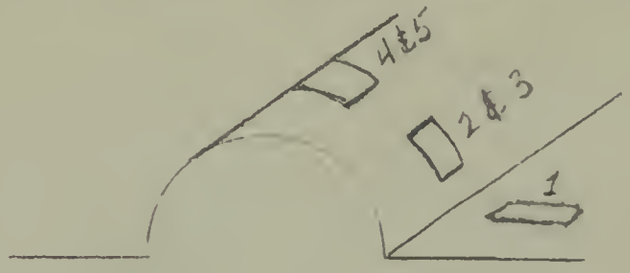

TABLE II

SPECIMEN NO. I

LOAD	P	δ_T	GAGE READINGS - Millivolts				
lbs	PSI	ELONG. x.10⁻³	1	2	3	4	5
1500	75	28	.117	2.355	2.271	.861	.836
2100	↓	27	.115	2.249	2.165	.831	.827
2400		26	.110	2.165	2.081	.805	.792
2700		25	.110	2.134	2.050	.787	.789
3000		24	.110	2.106	2.022	.775	.776
3300		22	.108	2.03	1.946	.745	.752
3600		21	.108	2.013	1.929	.738	.745
3900		20	.105	1.934	1.850	.712	.726
4500		19	.104	1.878	1.794	.674	.685
5100		18	.104	1.774	1.690	.644	.658
3300	100	31	.122	2.88	2.796	.943	.935
3900	↓	29.5	.119	2.70	2.616	.891	.935
4500		28	.111	2.613	2.529	.872	.908
5100		27.5	.112	2.755	2.671	.856	.891
5700		27	.111	2.575	2.491	.829	.876
6300		26	.105	2.462	2.378	.870	.857
5000	120	38	.146	3.422	3.338	1.230	1.122
6800	↓	35	.139	3.265	3.181	1.152	1083
8000		33	.134	3.075	2.991	1.075	1.043
9800		28	.122	2.791	2.707	0.950	0.943
11000		25	.115	2.610	2.526	0.874	0.896
13500		19	.108	2.220	2.136	0.720	0.795
16000	↓	11	.089	1.790	1.710	0.563	0.682
16000	180	35	.140	3.641	3.586	1.229	1.196
20000	↓	23	.115	3.113	2.556	0.950	0.975
24000		11	.100	2.462	1.776	0.704	0.780
20000		36.5	.140	3.960	3.704	1.327	1340
22000		31	.130	3.685	3.337	1.217	1.231
26000		20	.111	3.047	2.576	0.976	1.028
30000	↓	10	.090	2.379	1.902	0.701	0.775

TABLE II (CONT.)

SPECIMEN NO. 1

LOAD	P	δ_T	GAGE READINGS - MILLIMETERS				
lbs	PSI	INCHES $\times 10^{-3}$	1	2	3	4	5
30000	300	36	0.147	4.050	3.800	1.454	1.523
32000		31.5	.135	3.773	3.425	1334	1.477
36000		21.0	.112	3 1??	2.649	1.092	1.216
40000		10.5	.092	2 531	1.824	0.832	0.981
43000	400	35.5	.140	4.257	3.859	1.540	1.643
45000		31	.125	3.985	3391	1 431	1 511
49000		21	.110	3.431	2.635	1.196	1.362
54000		6	.070	2 718	1.900	0.912	1.170
58000	500	46.5	.164	4.362	3.506	1.513	1.940
60000		42.5	.152	4.088	3.130	1.730	1.891
64000		32.5	.130	3.476	2 303	1.528	1.720
69000		14.5	.100	2.802	0.14	1152	1 343
83000	600	10	.100	2.796		1.130	1.371
78000		23	.115	3.519	2.137	1402	1.570
76000		28	.120	3.852	2.571	1.520	1.689
72000		37	.132	4.377	3.303	1.075	2.110
70000		44	.141	4.628	3.703	1.830	2.720
67000		52	.150	4 889	4.138	1.912	2.435
64000		65	.152	2.868	4.775	2.253	2.690

TABLE II (CONT.)

SPECIMEN No. 2

LOAD	P	OT	GAGE READINGS — MILLIONTHS							
LBS	PSI	[illegible]	1	2	3	4	5	6	7	8
14500	100	-1.5	.062	.108	.155	.145	—	—	—	—
27500	200	-2.5	.320	.253	.315	.212	—	.037	—	—
40250	300	-4.0	.477	.391	.473	.318	—	.12	—	—
53250	400	-4.5	.655	.558	.642	.443	—	.125	—	—
66200	500	-6.5	.040	.921	1.021	.752	—	.125	—	—
11450	100	+5.5	.329	.371	.405	.462	.198	.311	.283	.300
24550	200	8.0	.668	.633	.563	.557	.152	.314	.245	.265
37600	300	6.5	.825	.822	.718	.659	.146	.338	.242	.249
50250	400	5.0	.972	.967	.861	.765	.100	.400	.241	.241
62000	500	10.5	1.140	1.268	1.087	.943	.337	.626	.455	.413
8750	100	18.5	.531	.733	.195	.442	.502	.669	.714	.631
21675	200	20.5	.681	.882	.355	.550	.514	.738	.757	.683
34150	300	19.0	.832	1.020	.525	.666	.526	.740	.765	.676
46900	400	17.5	.983	1.155	.681	.770	.529	.828	.756	.641
59400	500	19.5	1.128	1.336	.862	.901	.581	.917	.810	.692
7200	100	28.5	.344	.615	—	.074	.713	1.001	.239	1.007
19250	200	28.0	.488	.757	.024	.197	.703	1.042	.259	1.022
31900	300	28.5	.637	.891	.208	.306	.719	1.105	.281	1.022
44400	400	30.0	.771	1.018	.372	.434	.785	1.202	.334	1.070
56800	500	30.0	.897	1.138	.547	.547	.796	1.252	.342	1.052
69000	600	30.0	1.011	1.242	.700	.661	.834	1.334	.378	1.073

TABLE II (CONT.)

SPECIMEN No. 2

LOAD	P	δ_T	GAGE READINGS — MINUTES							
lbs	PSI	E-9 x.10-3								
5400	100	36.5	—	.134	—	—	711	1.350	1.884	1.175
18000	200	37.5	0	.251	—	—	841	1.368	1.944	1.251
30900	300	40.0	.151	.400	—	—	951	1.400	1.998	1.322
42800	400	40.75	.267	.480	.015	—	9.5	1.468	2.031	1.245
55400	500	39.0	.400	.548	.251	—	9.0	1.490	2.080	1.205
67700	600	34.5	.531	.720	.415	.104	432	1.532	2.102	1.178
5700	100	45.25	-.272	.005	-.470	-.470	1.041	1.583	2.174	1.405
17350	200	47.75	-.022	.300	-.275	-.241	1.161	1.722	2.320	1.541
29550	300	50.25	.180	.508	-.078	-.192	1.127	1.852	2.431	1.667
41100	400	51.25	.342	.662	.157	-.074	1.310	1.921	2.511	1.694
57000	500	52.5	.550	.800	.316	+.064	1.361	2.022	2.556	1.737
[illegible]	600	51.5	.115	1.002	.513	+.205	1.712	[illegible]	2.745	1.765
14300	600	52.5	-.058	.321	.431	-.108	1.732	2.250	2.910	1.677
[illegible]	"	74.75	-.512	-.100	1.458	-.204	.711	3.931	5.720	1.305
62750	"	90.00	-.993	-.615	2.583	-.224	1.242	5.230	4.832	1.33
61450	"	113.00	-1.600	-1.382	4.306	-.168	3.142	6.513	6.717	3.715
[illegible]	"	140.00	-1.780	-1.863	5555	-.248	4.92	8.302	8.818	6.552
51,38	"	166.	-1.650	-2.172	6.400	-.362	6.310	10.743	10.62	8.142
5700	"	202	-.491	-2.502	8.141	-.624	4.305	13.358	2.733	9.77-1

TABLE II (CONT.)

SPECIMEN No. 1

LOAD	P	δ_T	STRESS - P.S.I.				
lbs	PSI	elong $\times 10^{-3}$	1	2	3	4	5
200	0	2.5	282	1100	1300	860	
800		5.5	436	2700	3310	1245	
1400		12.5	615	4250	5110	1670	
2000		15.0	757	5600	6850	1762	
3200		10.5	757	9800	10000	2720	
4400		21.5	936	13000	13300	3740	
5600		24.0	1130	16000	16580	5550	
6800		28.5	1372	18750	19000	6000	
8000		33.5	1500	22600	22400	15000	
450	25	19	822	16500	15600	6100	6540
900		16	873	16000	14750	5800	6300
1200		16	848	15300	13700	5600	6170
1500		15	873	15000	13300	5300	5920
1800		13	911	14200	12100	5100	5640
2100		14	911	13400	11300	4800	5400
2700		12	886	12000	10250	4200	5170
3300		9	886	10000	8600	3500	4810
450	50	23	1515	23700	23500	8500	9220
900		22	1154	21200	22200	8300	8450
1500		20	1180	20800	19800	7600	8100
1800		19	1180	20500	19400	7600	8020
2100		18	1145	19600	18300	7200	7700
2400		17.5	1283	19250	17900	7200	7611
3000		17	1310	18300	16600	6600	7440
3600		15	1245	17250	15250	6300	7200
4200		13.5	1220	16100	14400	5800	6680

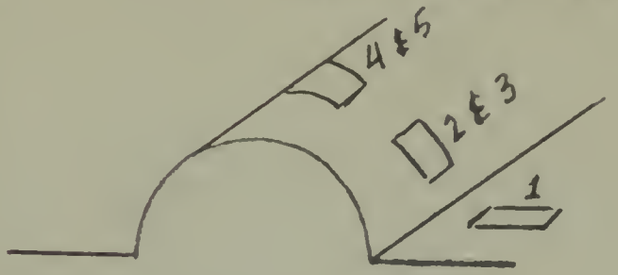

TABLE III

SPECIMEN NO. 1

LOAD	P	δ_T	STRESS — P.S.I.				
lbs	PSI	ELONG $\times 10^{-3}$	1	2	3	4	5
1500	75	28	1510	30200	24150	11000	10720
2100	↓	27	1475	28850	27800	10610	10630
2400		26	1410	27800	26700	10250	10180
2700		25	1410	27300	26300	10000	10100
3000		24	1410	27000	25700	9900	9970
3300		22	1375	26000	25000	9500	9650
3600		21	1335	25800	24750	9400	9560
3900		20	1350	24700	23750	9000	9310
4500		19	1335	24000	23000	8600	8790
5100		18	1335	22750	21700	8200	8450
3300	100	31	1506	37000	35520	12070	12000
3900	↓	29.5	1530	34710	33550	11470	12000
4500		28	1425	33500	32450	11200	11650
5100		27.5	1440	34100	34250	10800	11500
5700		27	1425	33000	32000	10500	11250
6300		26	1350	31600	30500	9780	11000
5000	120	38	1875	43500	43400	15800	14400
6800	↓	35	1785	41900	40800	14800	13900
8000		33	1720	39450	38400	13800	13400
9800		28	1566	35800	34950	12200	12100
11000		25	1480	33500	32400	11200	11500
13500		19	1388	25500	27400	9240	10200
16000		11	1040	22950	21450	7730	8750
16000	180	35	1795	48600	45400	15800	15350
20000	↓	23	1475	39900	12200	12500	
24000		11	1282	31600	9040	10000	
20000	220	36.5	1795	50800	47600	17350	16420
22000	↓	31	1670	42800	15600	15800	
26000		20	1410	33000	12530	13180	
30000		10	1150	22500	9000	9950	

TABLE III (CONT.)

SPECIMEN No. 1

LOAD	P	δ_T	STRESS - P.S.I.				
lbs	PSI	ELONG $\times 10^{-3}$	1	2	3	4	5
30000	300	36	1885	52100	45800	18650	19550
32000	↓	31.5	1730	48350	44000	17100	18300
36000		21.0	1440	40600	34000	14000	15600
40000		13.5	1180	32400	23400	10680	12660
43000	400	35.5	1800	54600	49500	19150	21100
45000	↓	31	1600	51200	43500	19400	19400
49000		21	1410	44000	33800	15350	17500
54000		6	894	34850	22500	11700	15000
58000	500	46.5	2100	56000	45000	23250	24900
60000	↓	42.5	1950	52400	40200	22200	24750
64000		32.5	1670	44550	29400	19600	22100
64000		14.5	1283	35450	10000	14800	17500
83000	600	10	1283	35400		14500	19800
78000	↓	23	1475	45200	27400	18000	20650
76000		28	1540	49500	33000	19500	21600
72000		37	1700	56200	42400	21500	23700
70000		44	1810	57400	47500	23500	34900
67000		51	1925	62800	53400	25400	31250
64000		6.5	1950	62500	57400	24300	34500

TABLE III (CONT.)

SPECIMEN NO 2.

LOAD	P	δ_T	STRESS - P.S.I.							
lbs	P.S.I.	elong $\times 10^{-3}$	1	2	3	4	5	6	7	8
14500	100	-1.5	796	1386	1990	1220	—	—	—	—
27500	200	-2.5	4110	3250	4040	2720	—	474	—	—
40250	300	-4.0	6120	5010	6080	4080	—	924	—	—
5325	400	-4.5	8410	7170	8280	5640	—	1603	—	—
66200	500	-6.5	13350	11800	13100	9650	—	1603	—	—
11400	100	+8.5	6790	7330	5460	5970	2540	3940	3055	3359
24550	200	8.0	8580	8770	7240	7150	1950	4100	3143	3148
37600	300	6.5	10580	10557	9230	8460	1870	4570	3110	3182
50250	400	5.0	12460	12400	11150	9830	2125	5130	3145	3403
62000	500	10.5	15780	16250	13130	12500	4350	8040	5870	5832
8750	100	18.5	6790	9400	2590	5870	6430	8540	9170	8100
21075	200	20.5	8840	11300	4560	7160	6660	4480	9720	8360
34150	300	19.0	10670	13100	6740	8560	6760	10120	9820	8845
46900	400	17.5	12600	14810	8750	9880	6950	10620	9710	8860
59400	500	14.5	14470	17120	11050	11650	7450	11750	10400	9670
7200	100	28.5	4160	7840	—	450	4150	12850	15870	12442
19250	200	28.0	6270	9710	308	2530	9020	13380	16130	12860
31900	300	28.5	8170	11420	7670	3430	9220	14180	16430	13237
44400	400	30.0	9900	13040	5030	5570	10150	15500	17350	14162
56800	500	30.0	11500	14610	7020	7070	10200	16050	17200	14735
69000	600	30.0	12480	15420	8980	8440	10750	17100	17660	12320

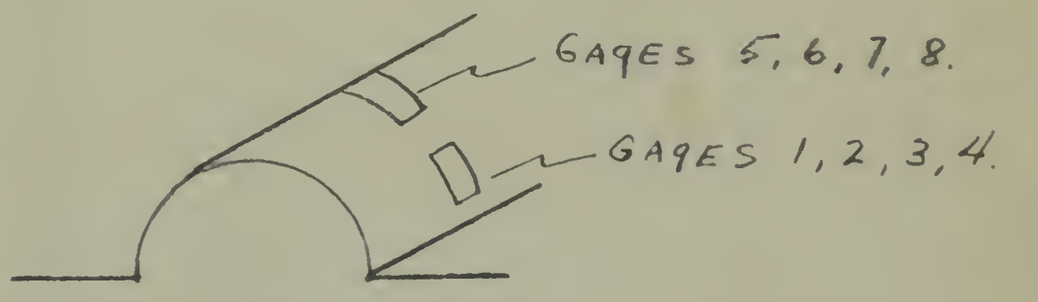

TABLE III (CONT.)

SPECIMEN NO 2

LOAD	P	δ_T	STRESS – P.S.I.							
lbs	PSI	FIONS ×10⁻³	1	2	3	4	5	6	7	8
5900	100	30.5	—	1783	—	—	10000	16540	24150	15080
18000	200	34.5	0	3220	—	—	10370	17470	25620	16050
30900	300	40	2015	5140	—	—	11020	17950	25610	15670
42800	400	40.75	3430	6170	1090	—	11600	18800	26020	15970
55800	500	39	5140	7680	3220	—	11620	19100	25650	15450
67700	600	39.5	6820	9250	5330	1400	11970	19650	25700	15300
5900	100	45.25	-3490	64.2	-6030	-6030	13450	20630	27900	18800
17850	200	47.75	-282	3850	-2882	-3730	15000	22000	29800	20410
29550	300	50.25	2310	6520	-359	-7210	14450	23800	31250	21410
41700	400	51.25	4260	8490	2018	-950	16800	24650	31950	21650
54000	500	52.5	7060	11050	4950	+872	17800	25900	32800	22300
66500	600	51.5	9160	12870	7350	+2630	18000	25750	32650	21850
64300	"	62.5	-7444	4110	8170	-1385	22000	28550	38400	21500
64000	"	74.75	-6780	-1283	18700	-3385	24900	50500	47700	17500
62750	"	90.0	-12730	-7890	33200	-2870	29400	67800	62000	17070
61750	"	113	-20500	-17770	52300	-2155	40900	85500	85200	47500
60200	"	140.	-22810	-23400	71200	-3180	63200	111360	113200	84000
58750	"	166	-21200	-27400	81200	-4720	87200	137400	136700	104000
57000	"	202.	-12800	-32150	104800	-8000	120000	171200	164500	125500

TABLE III (CONT.)

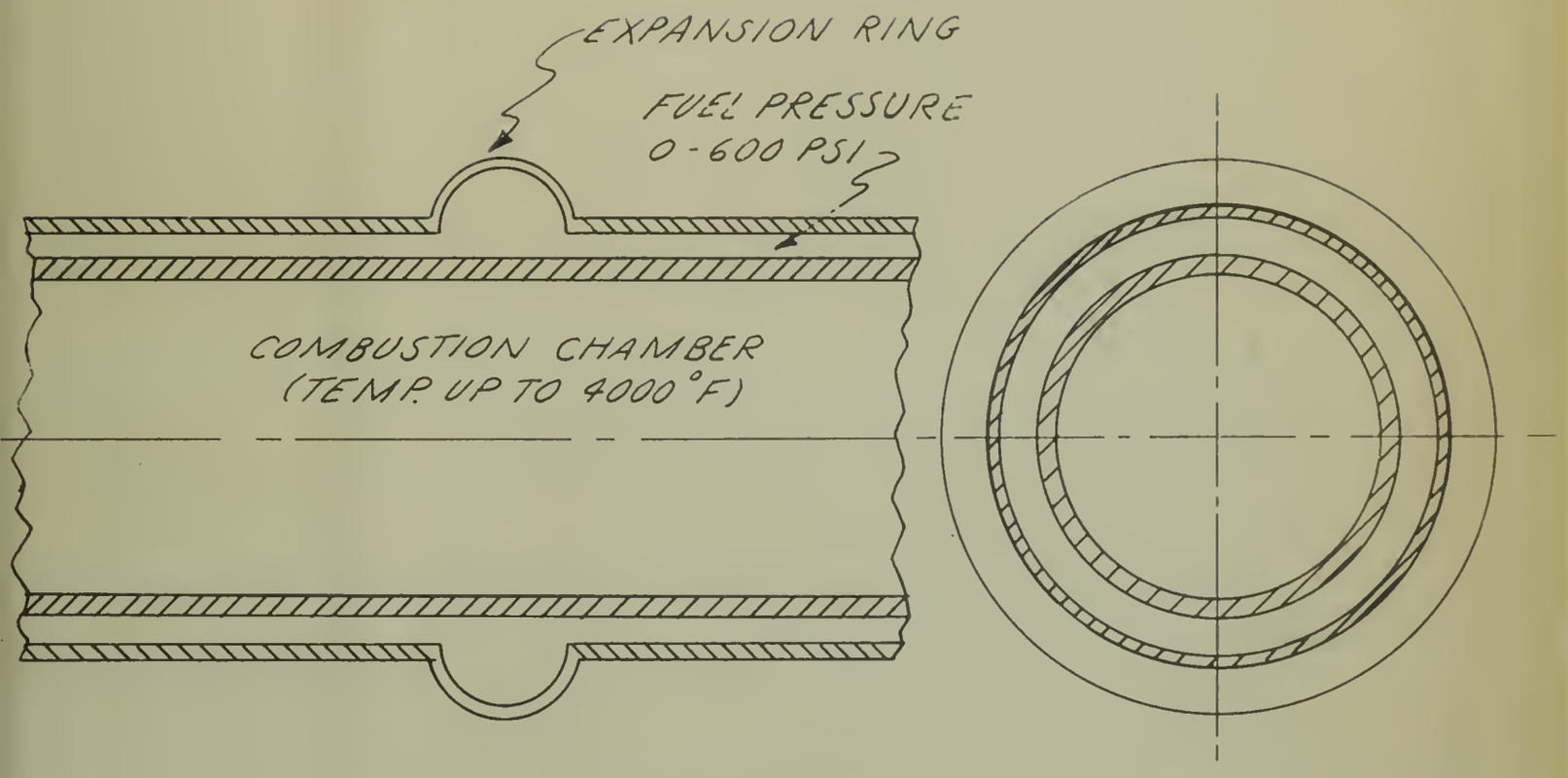

ROCKET SECTION

THE FOLLOWING TEMPERATURE DISTRIBUTION IS ASSUMED:

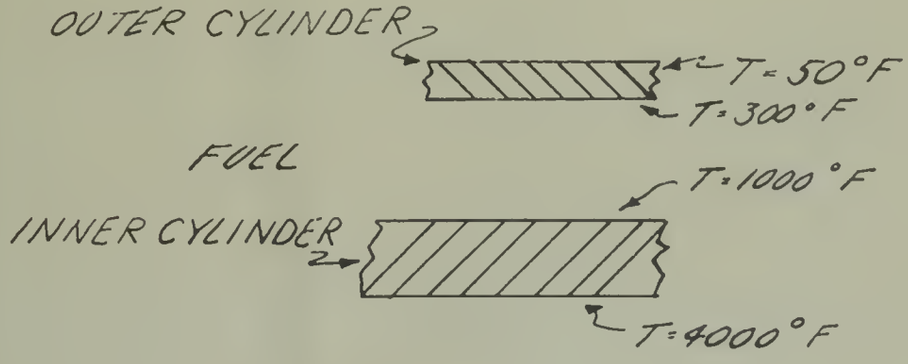

FIG. 1

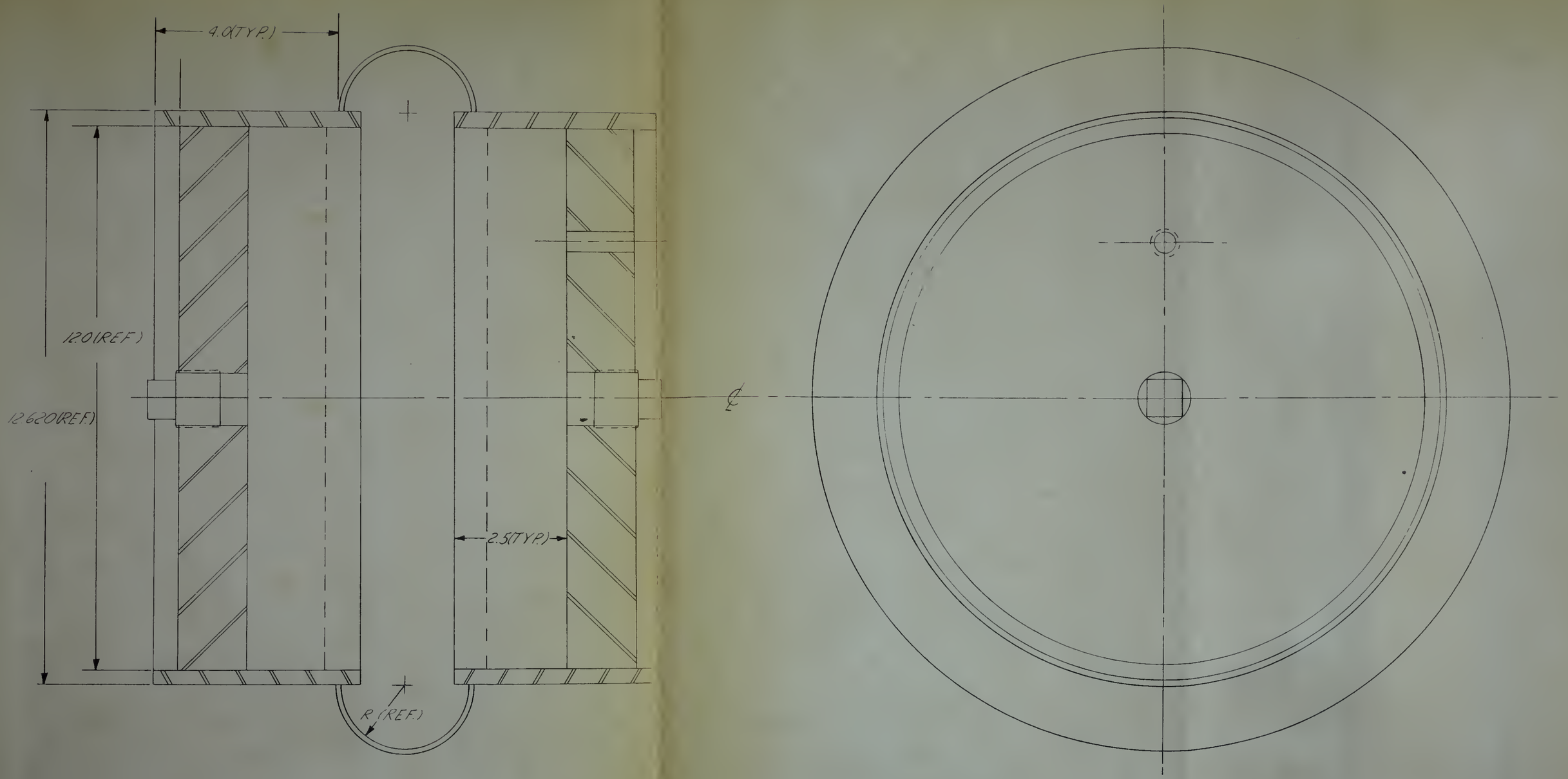

FIG. 2

SCALE: 1/2

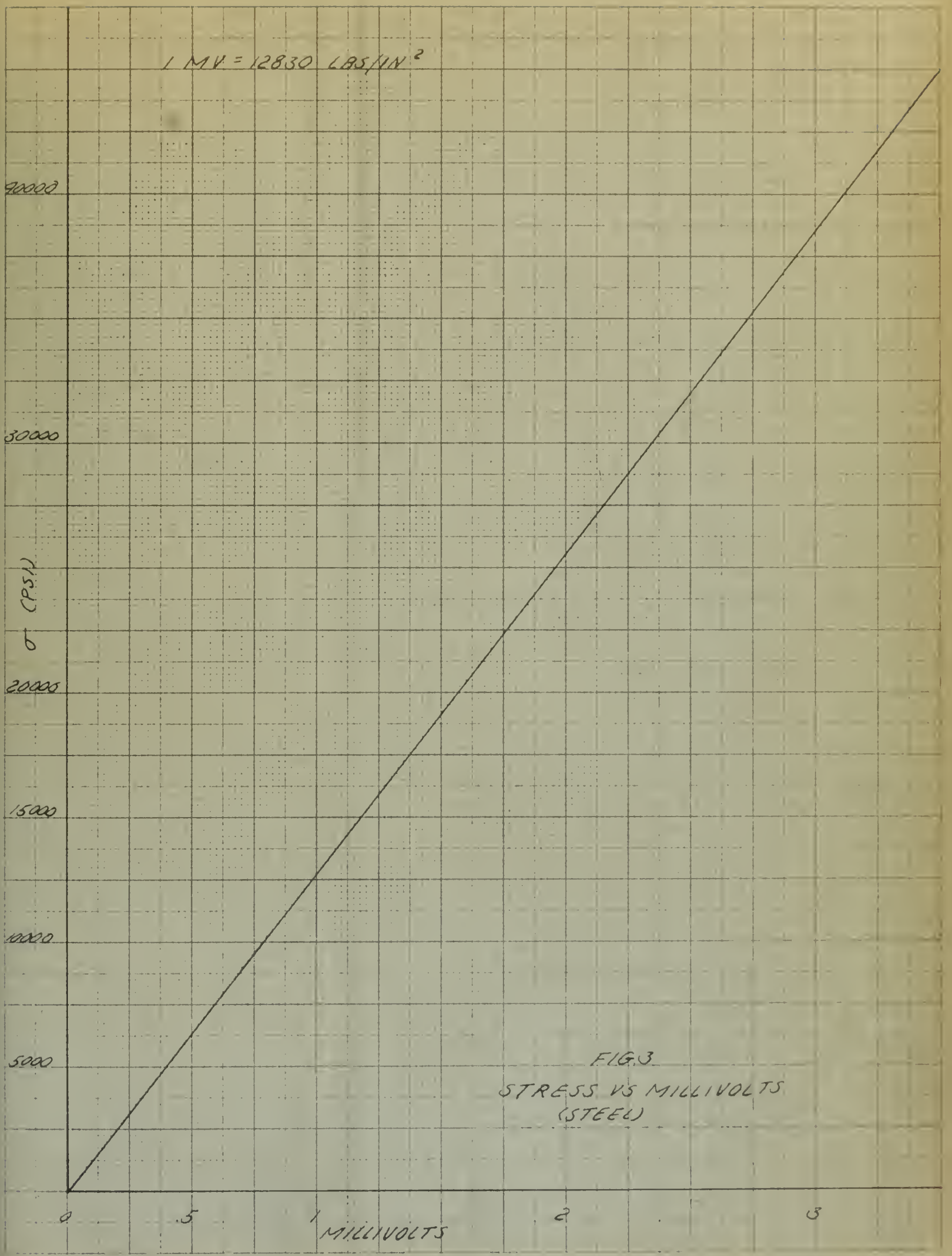

FIG. 3
STRESS VS MILLIVOLTS
(STEEL)

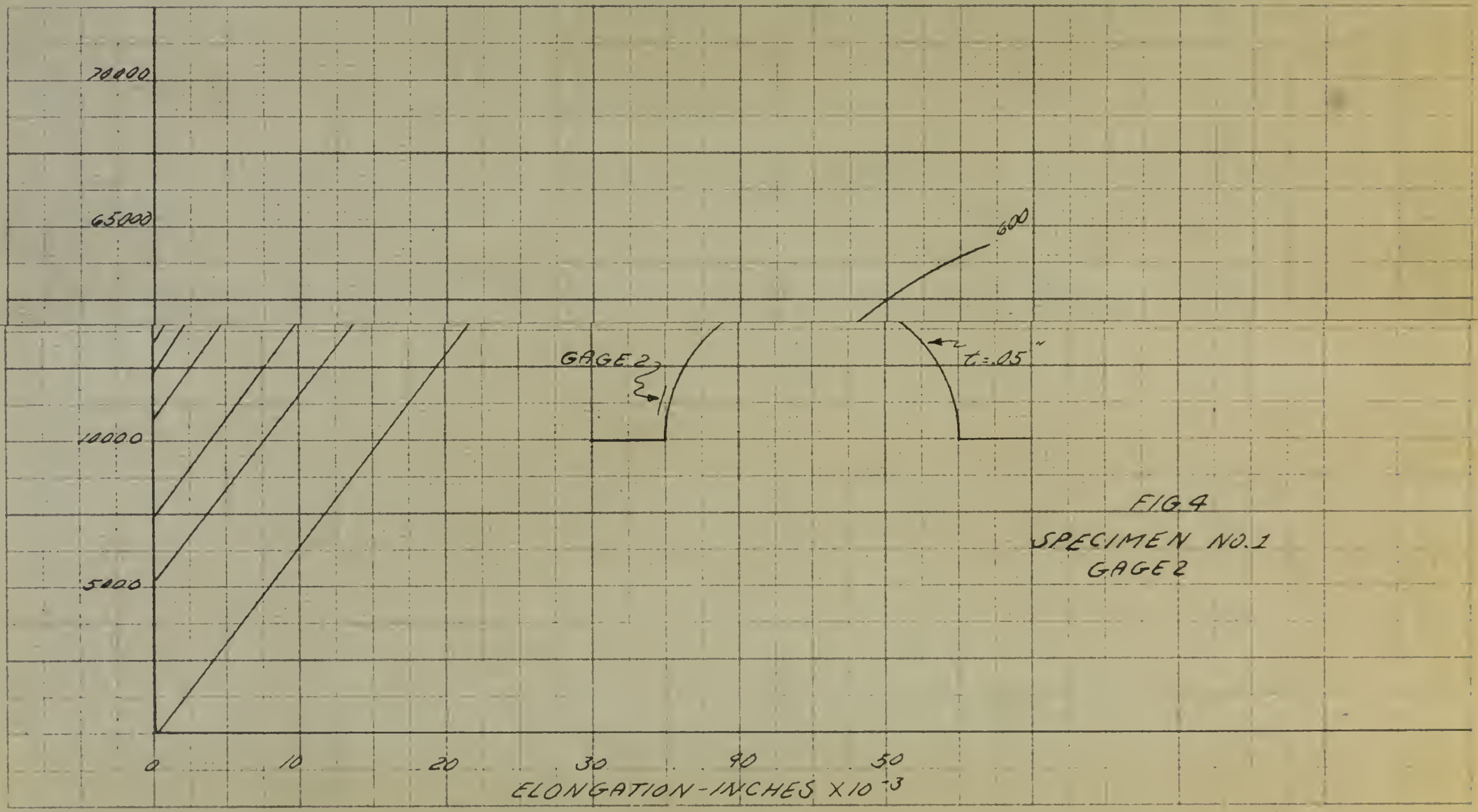

FIG 4
SPECIMEN NO. 1
GAGE 2

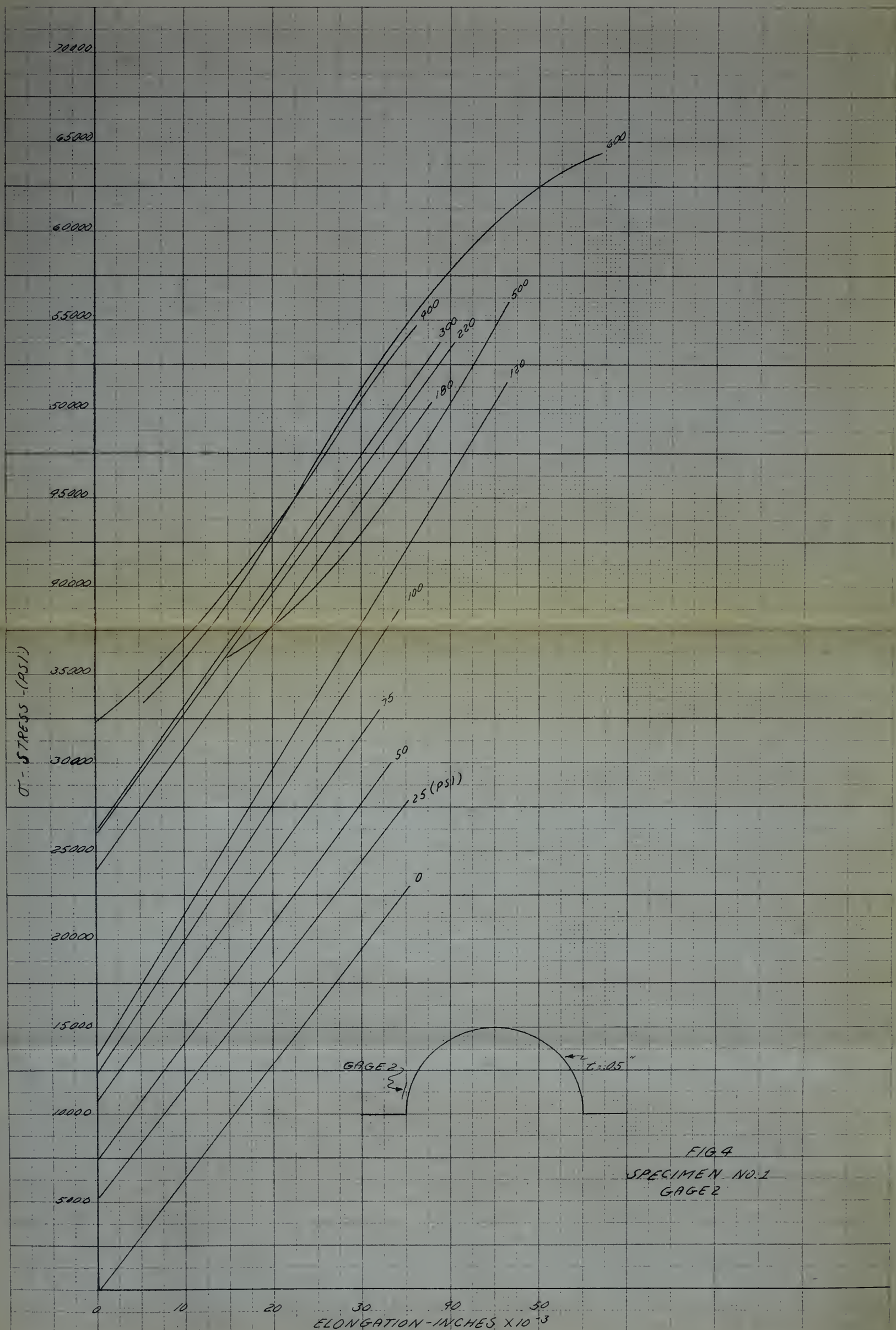

FIG 4
SPECIMEN NO. 1
GAGE 2

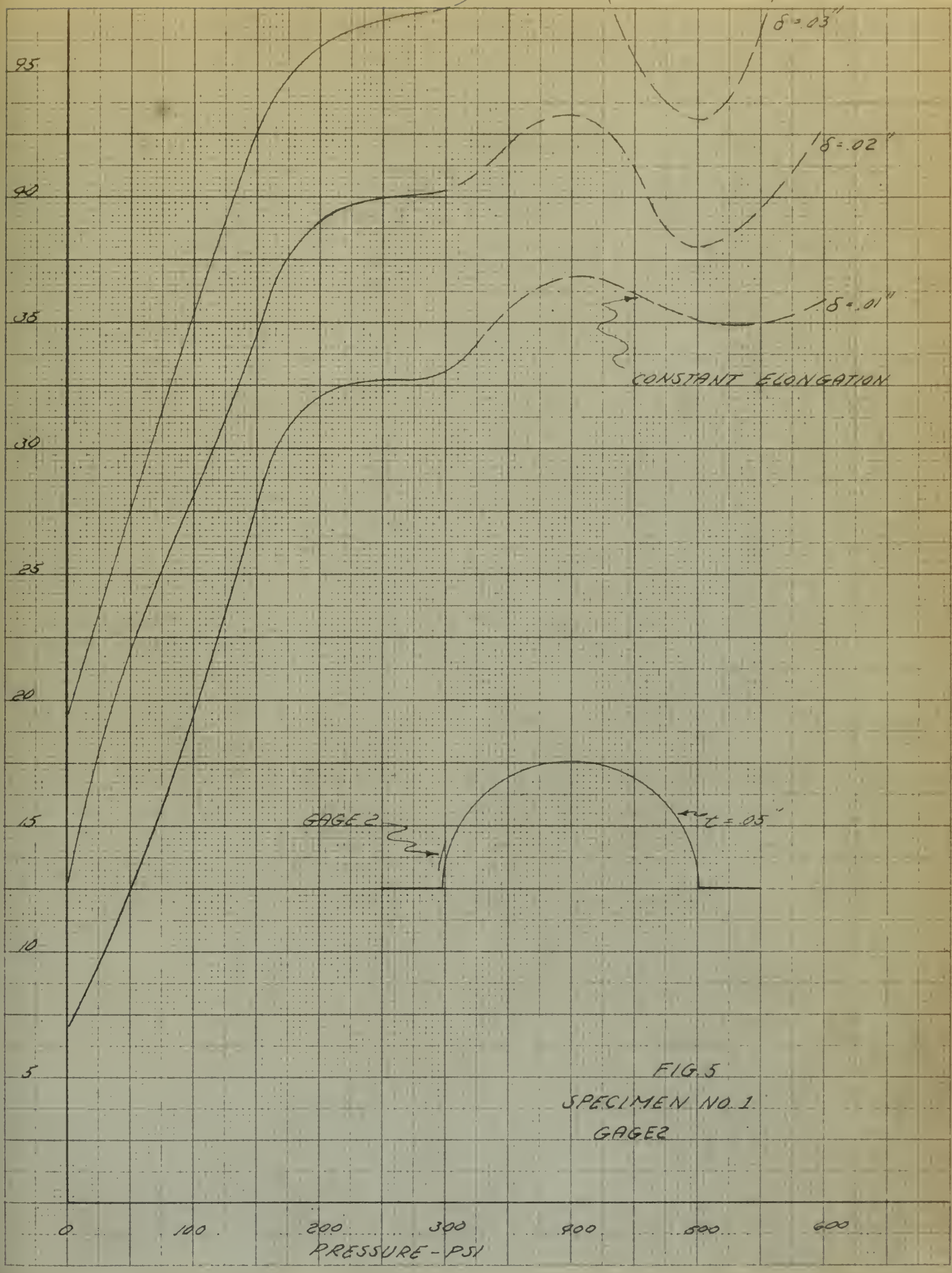

FIG. 5
SPECIMEN NO. 1
GAGE 2

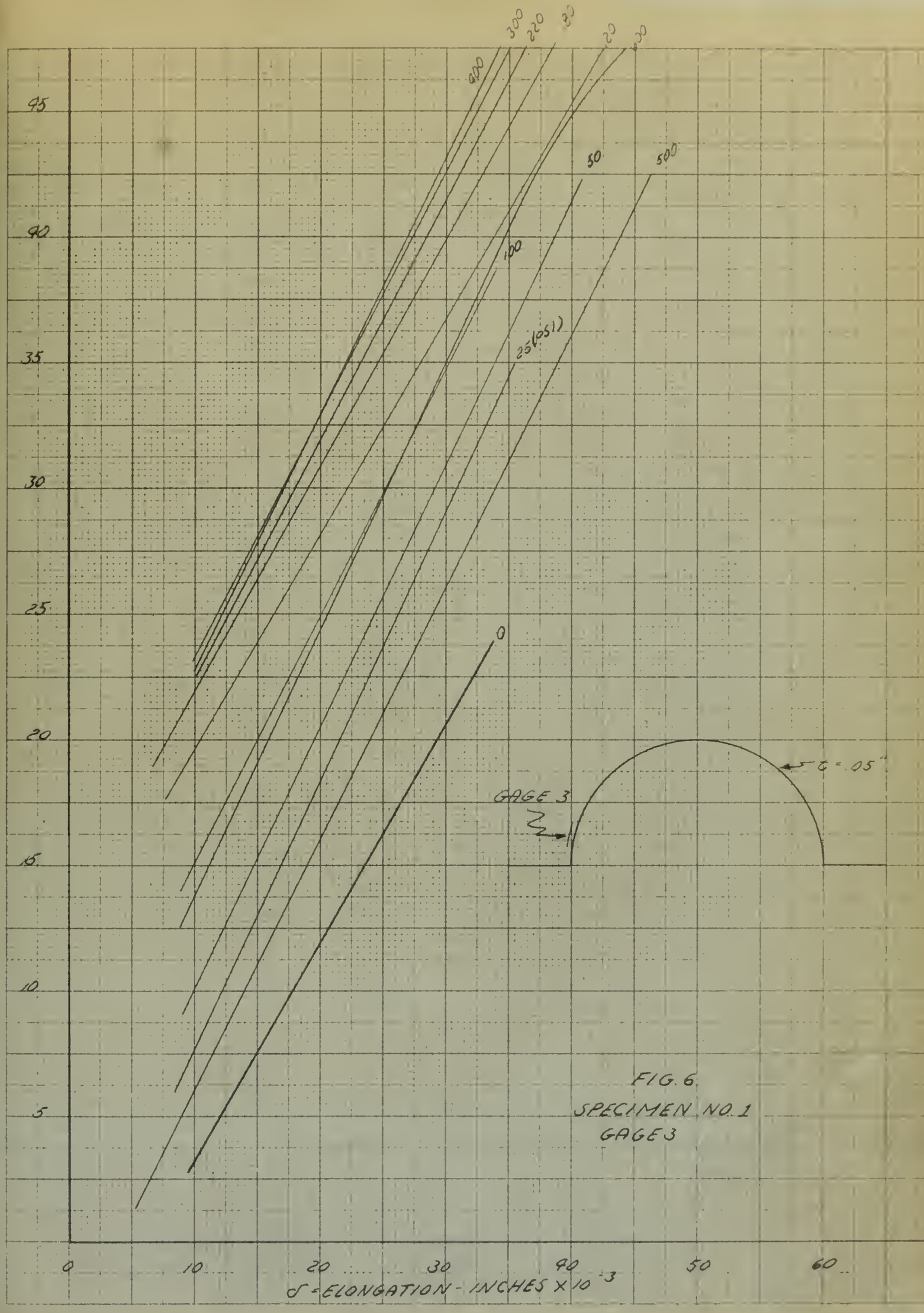

FIG. 6
SPECIMEN NO. 1
GAGE 3

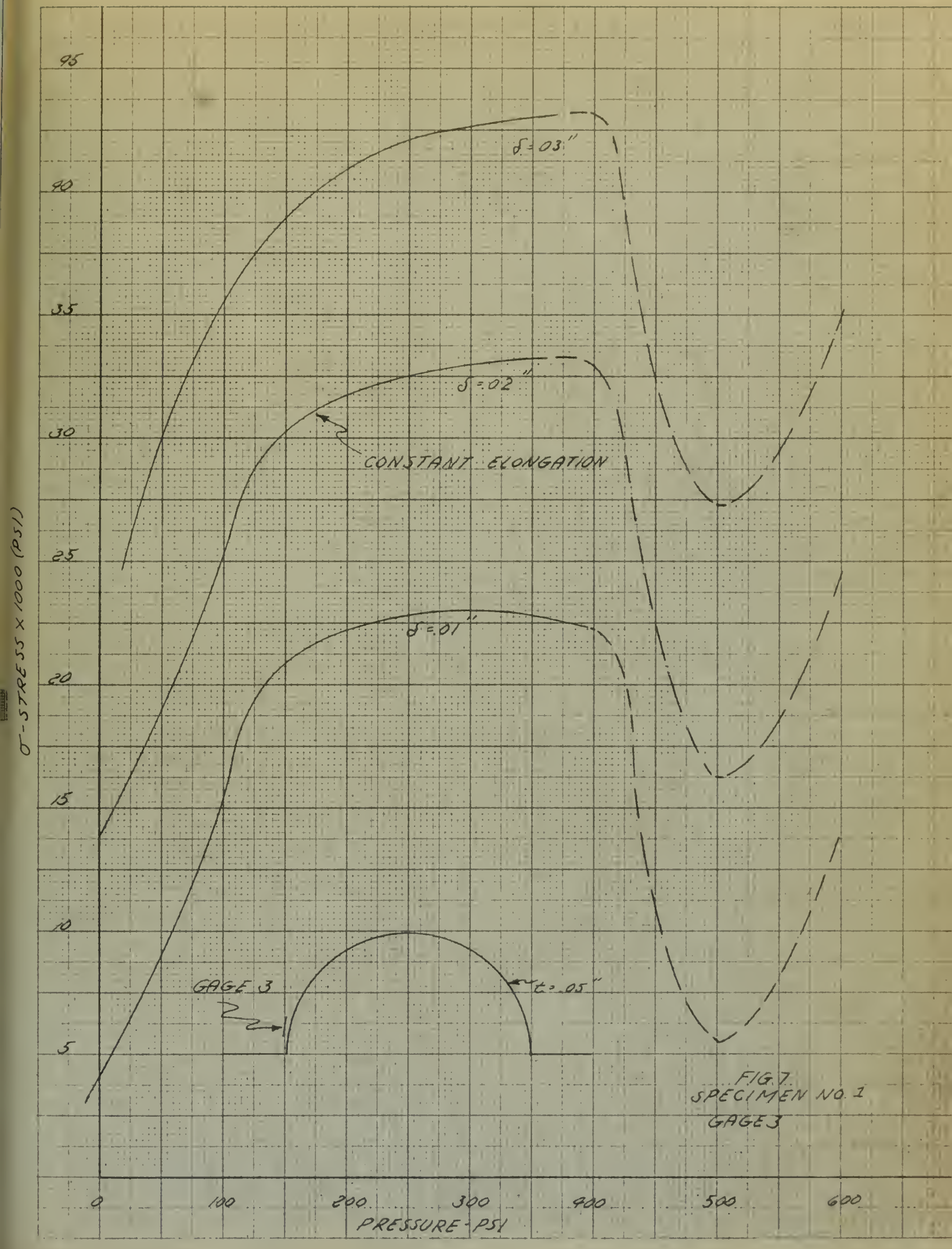

FIG. 7
SPECIMEN NO. 1
GAGE 3

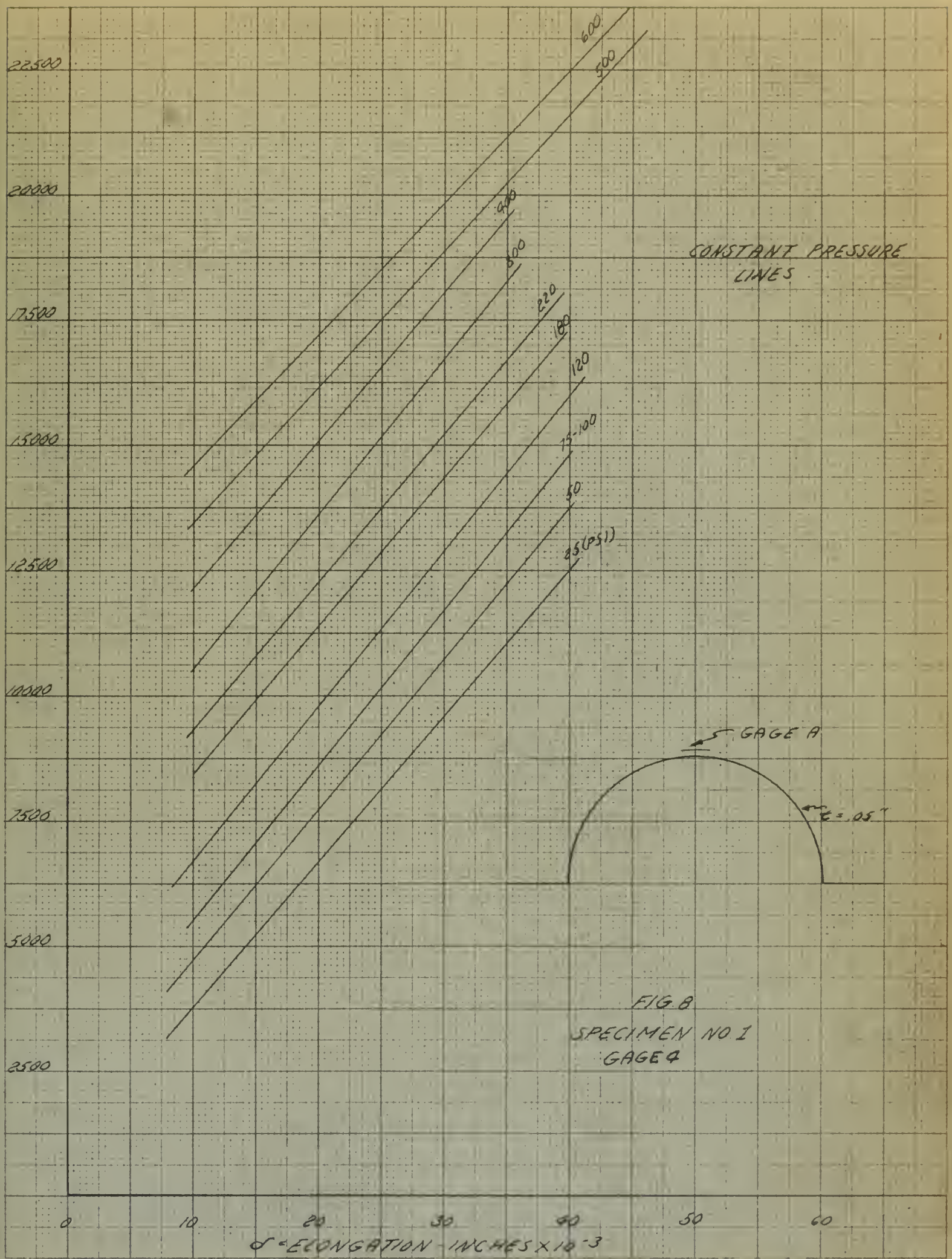

FIG 8
SPECIMEN NO 1
GAGE 4

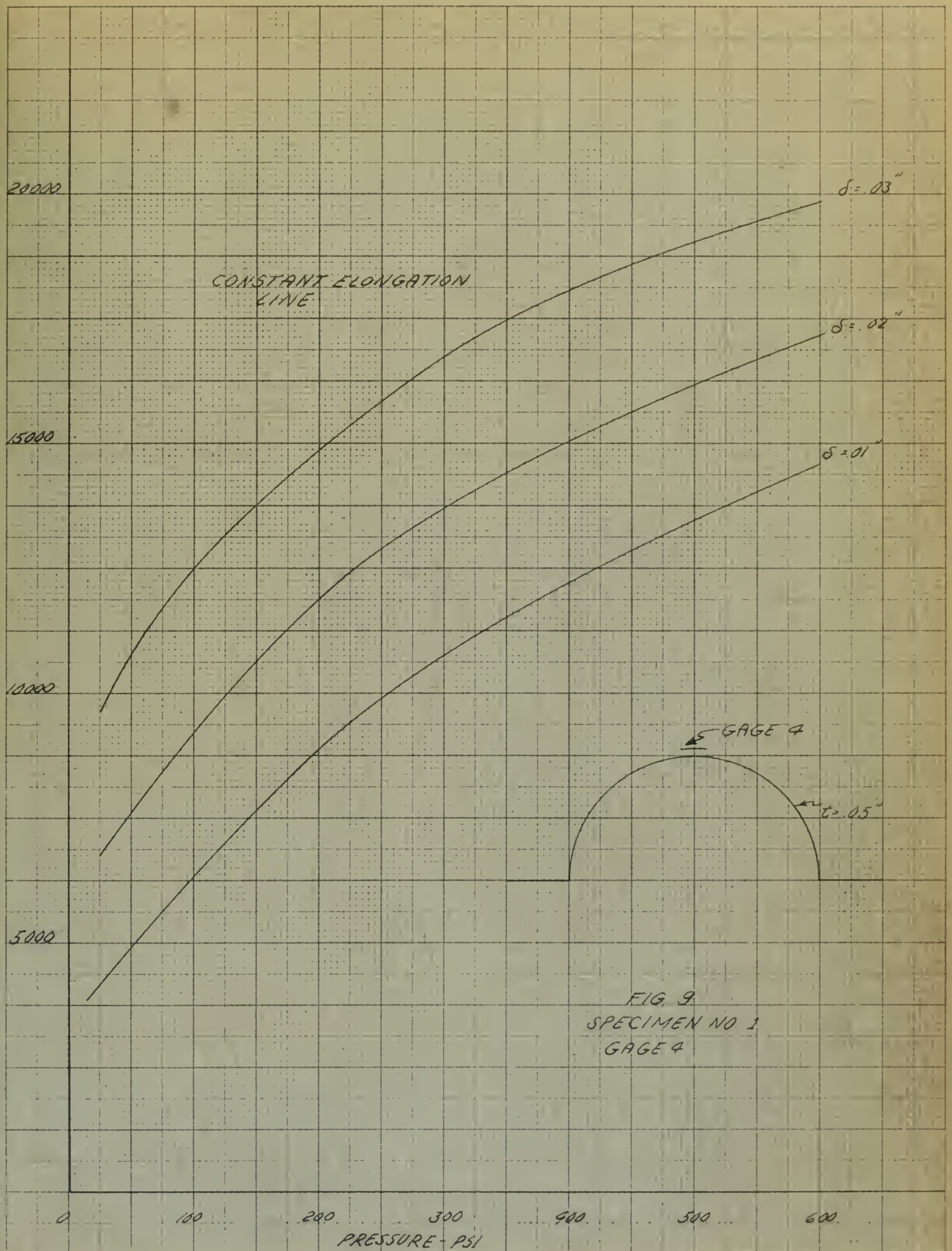

FIG. 9
SPECIMEN NO. 1
GAGE 4

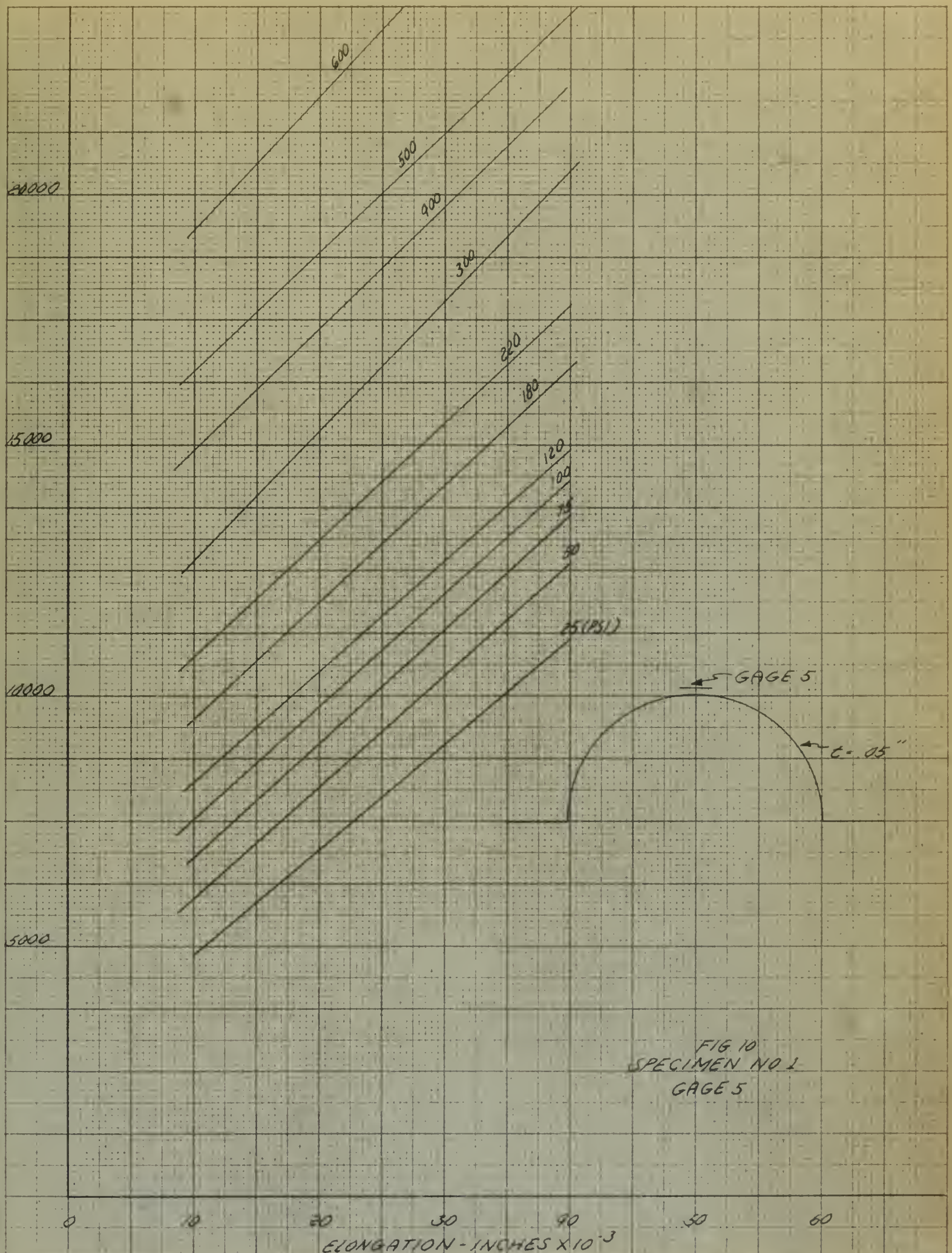

FIG 10
SPECIMEN NO 1
GAGE 5

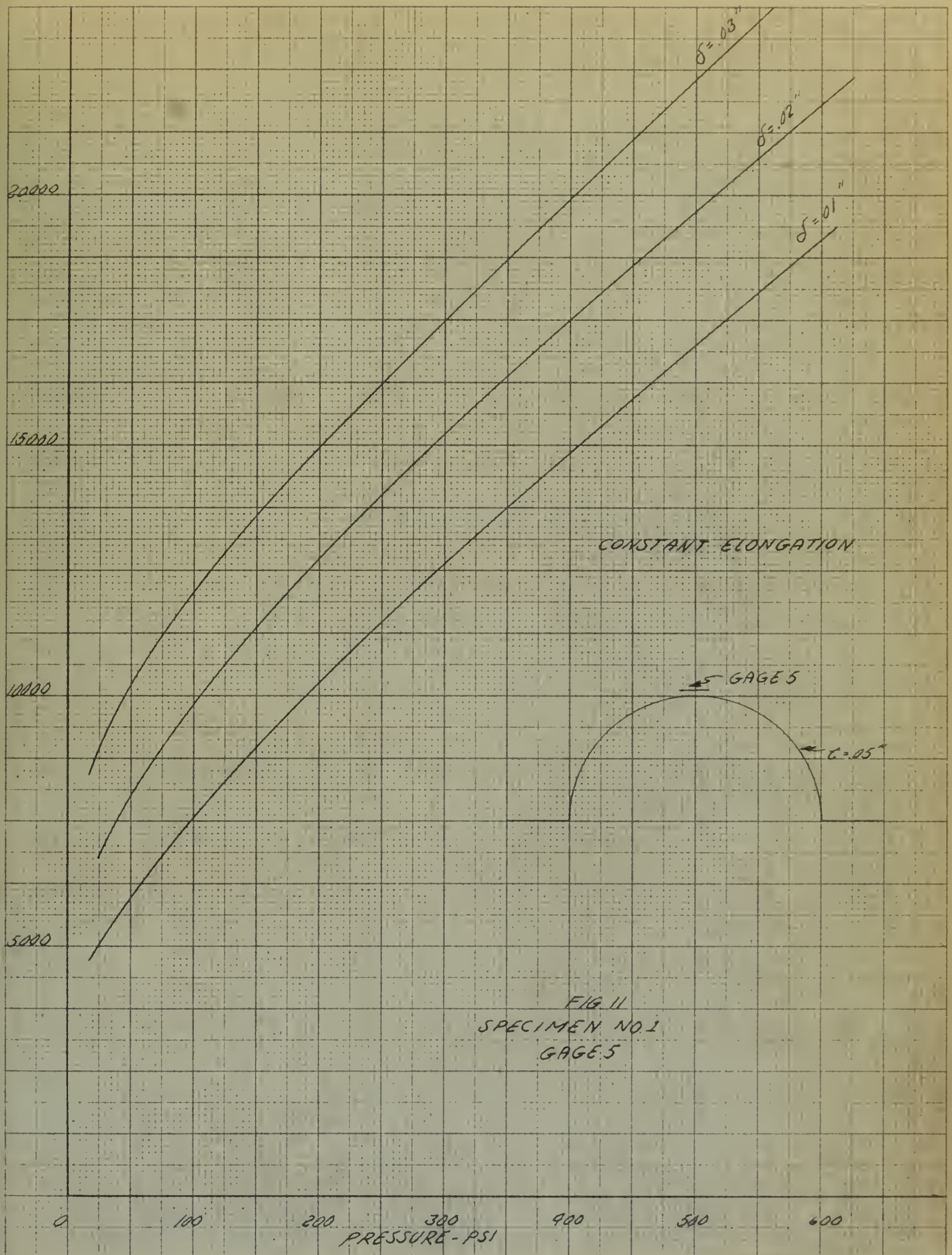

FIG. 11
SPECIMEN NO. 1
GAGE 5

FIG. 12
SPECIMEN NO. 2
GAGE 1

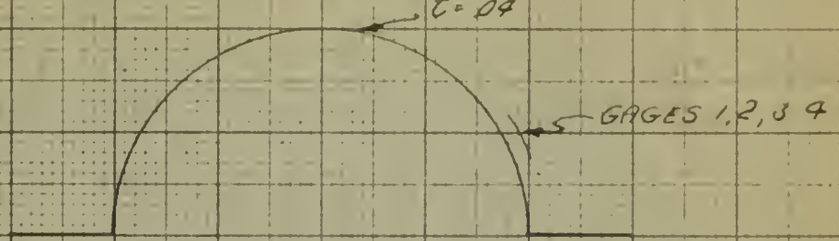

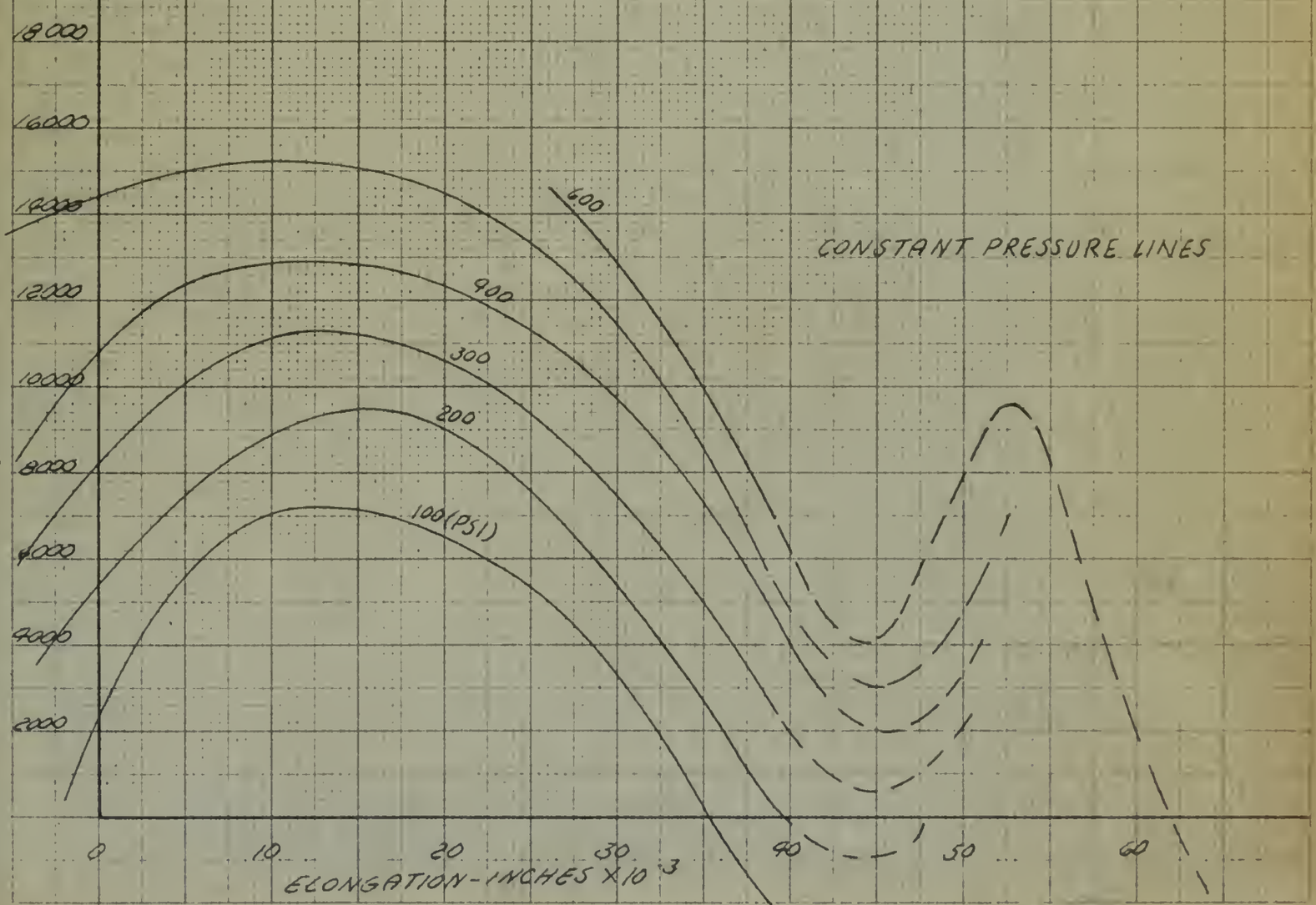

FIG. 13

SPECIMEN NO. 2

GAGE 2

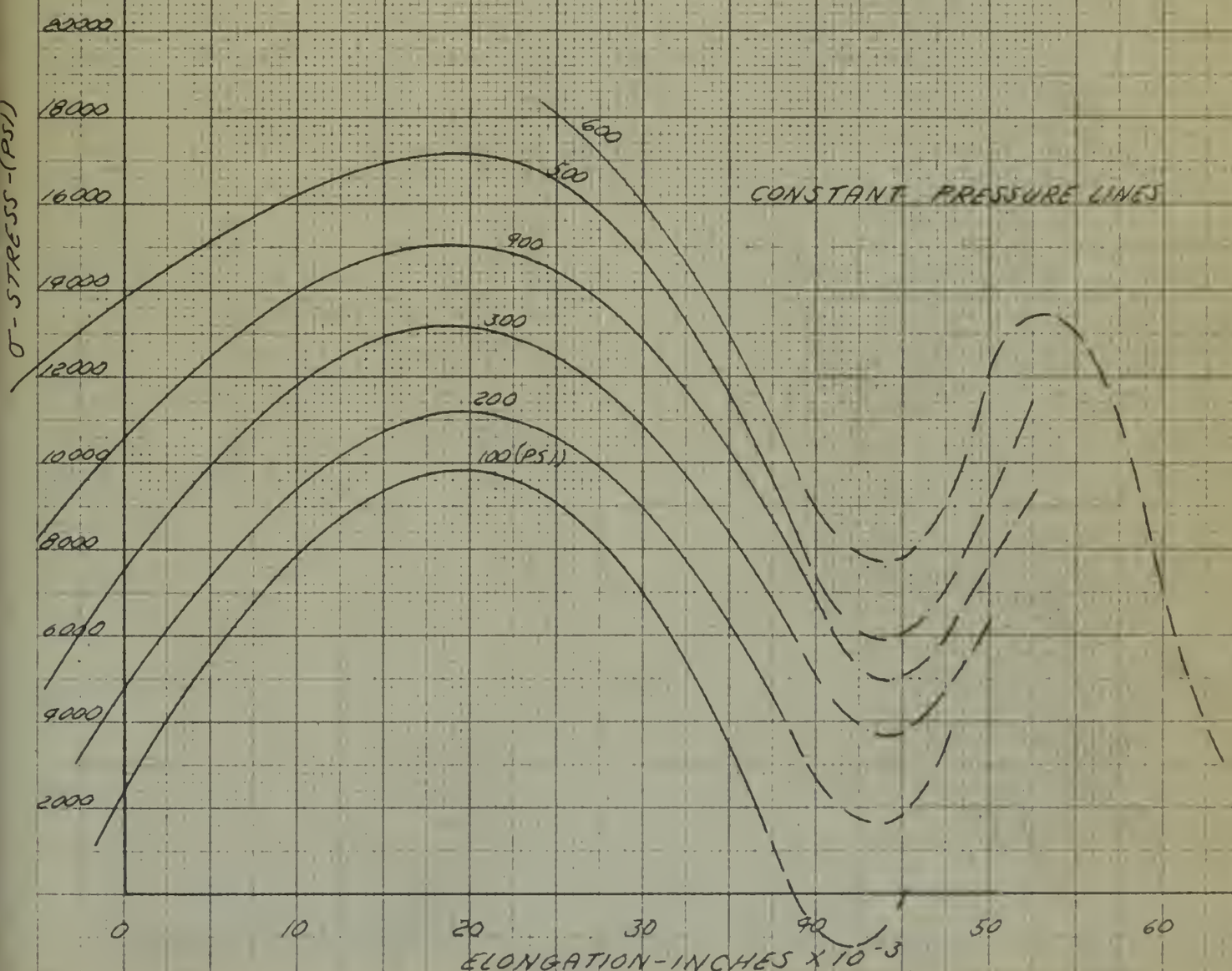

FIG. 19
SPECIMEN NO. 2
GAGE 3

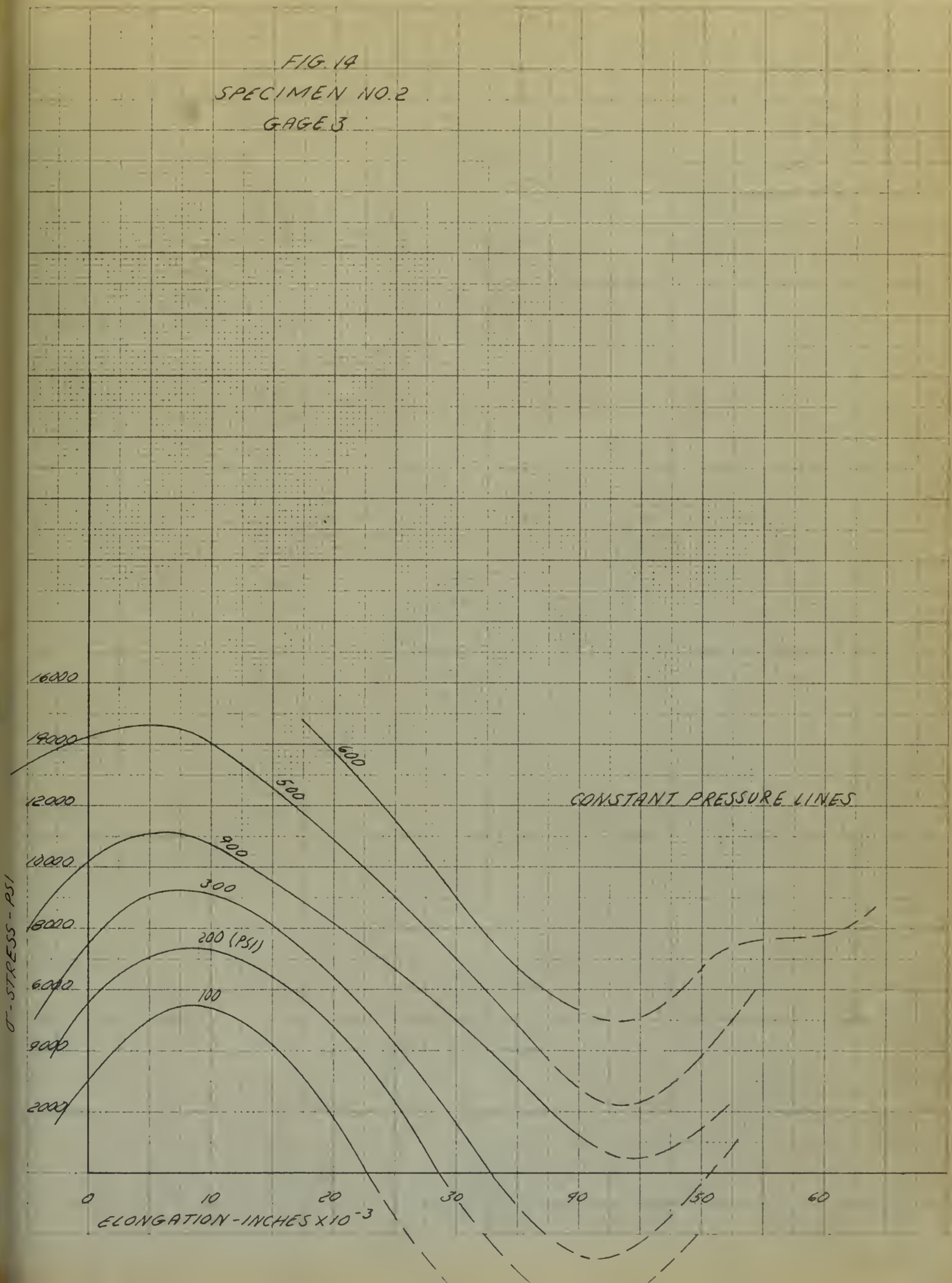

FIG. 15
SPECIMEN NO. 2
GAGE 4

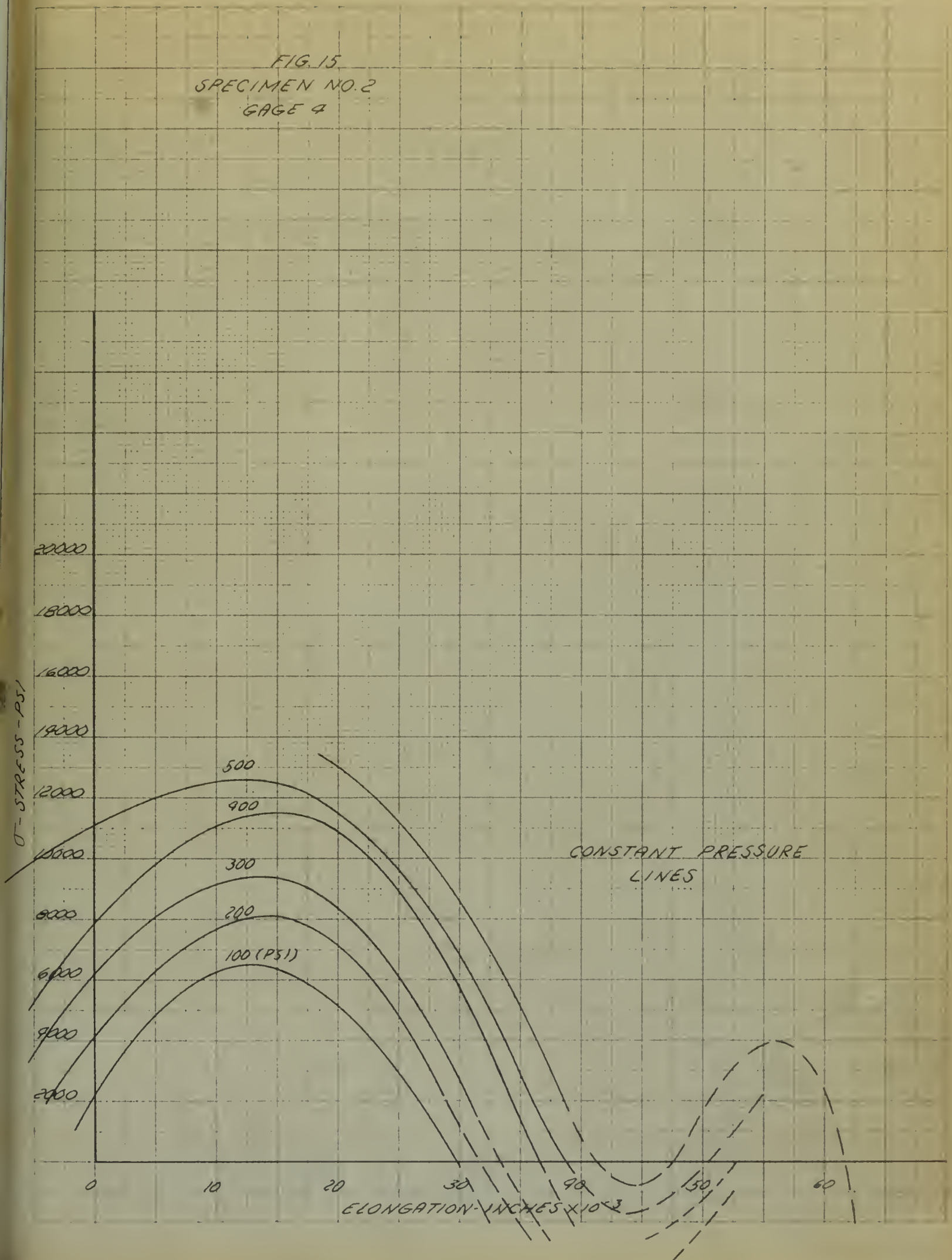

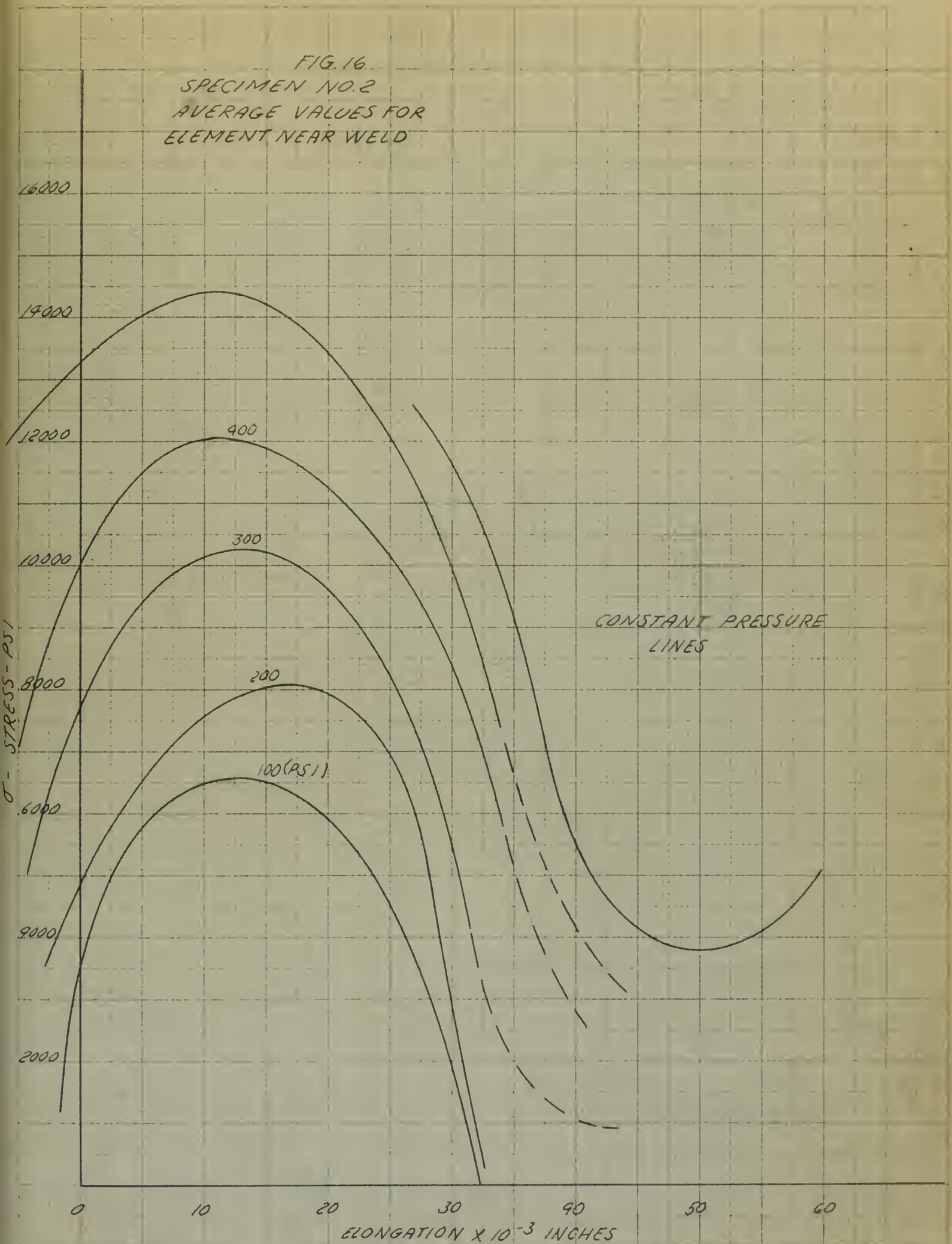
FIG. 16.
SPECIMEN NO. 2
AVERAGE VALUES FOR
ELEMENT NEAR WELD
16000
14000
12000
10000
8000
6000
9000
2000
400
300
200
100 (PSI)
CONSTANT PRESSURE
LINES
σ - STRESS - PSI
0
10
20
30
40
50
60
ELONGATION X 10⁻³ INCHES

FIG. 17
SPECIMEN NO. 2
GAGE 5

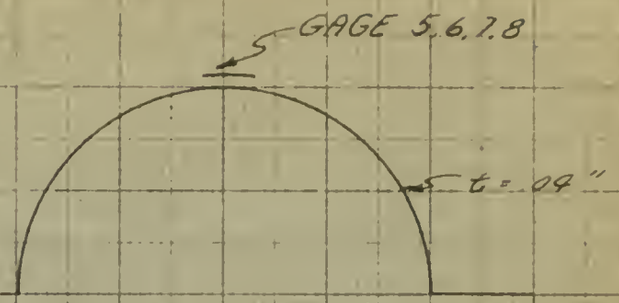

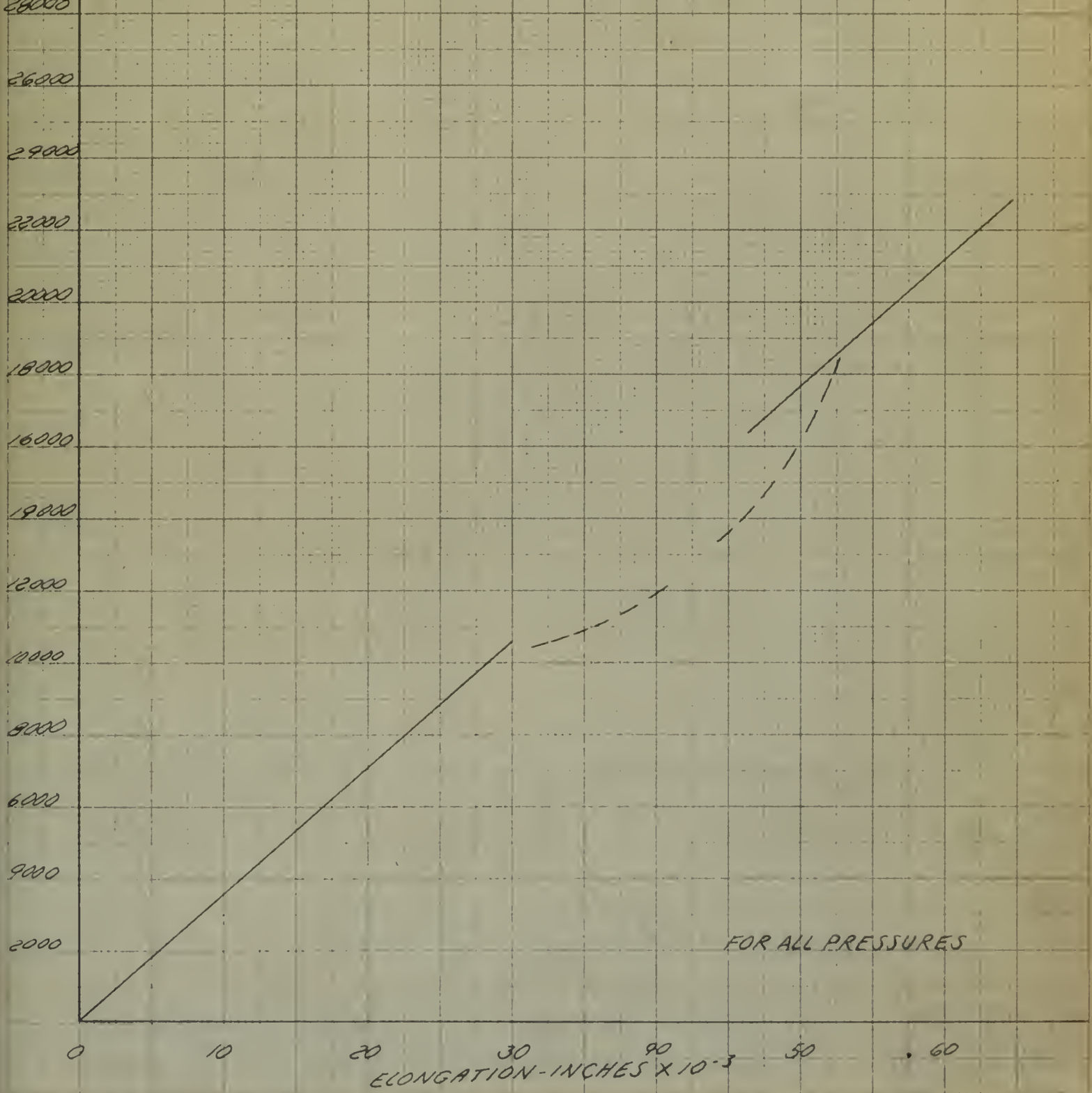

σ - STRESS - PSI

FIG. 18
SPECIMEN NO. 2
GAGE 6

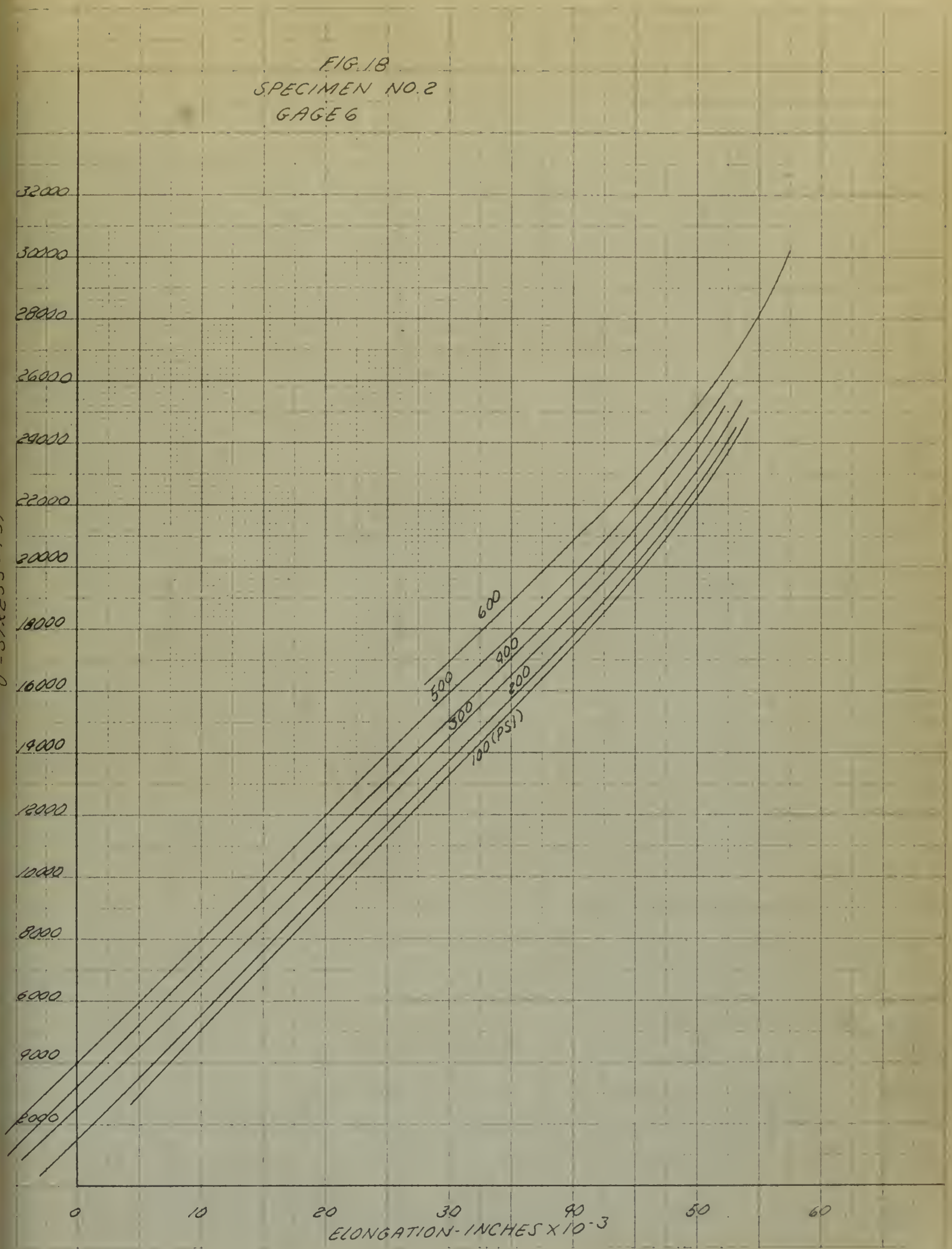

FIG 19
SPECIMEN NO. 2
GAGE 7

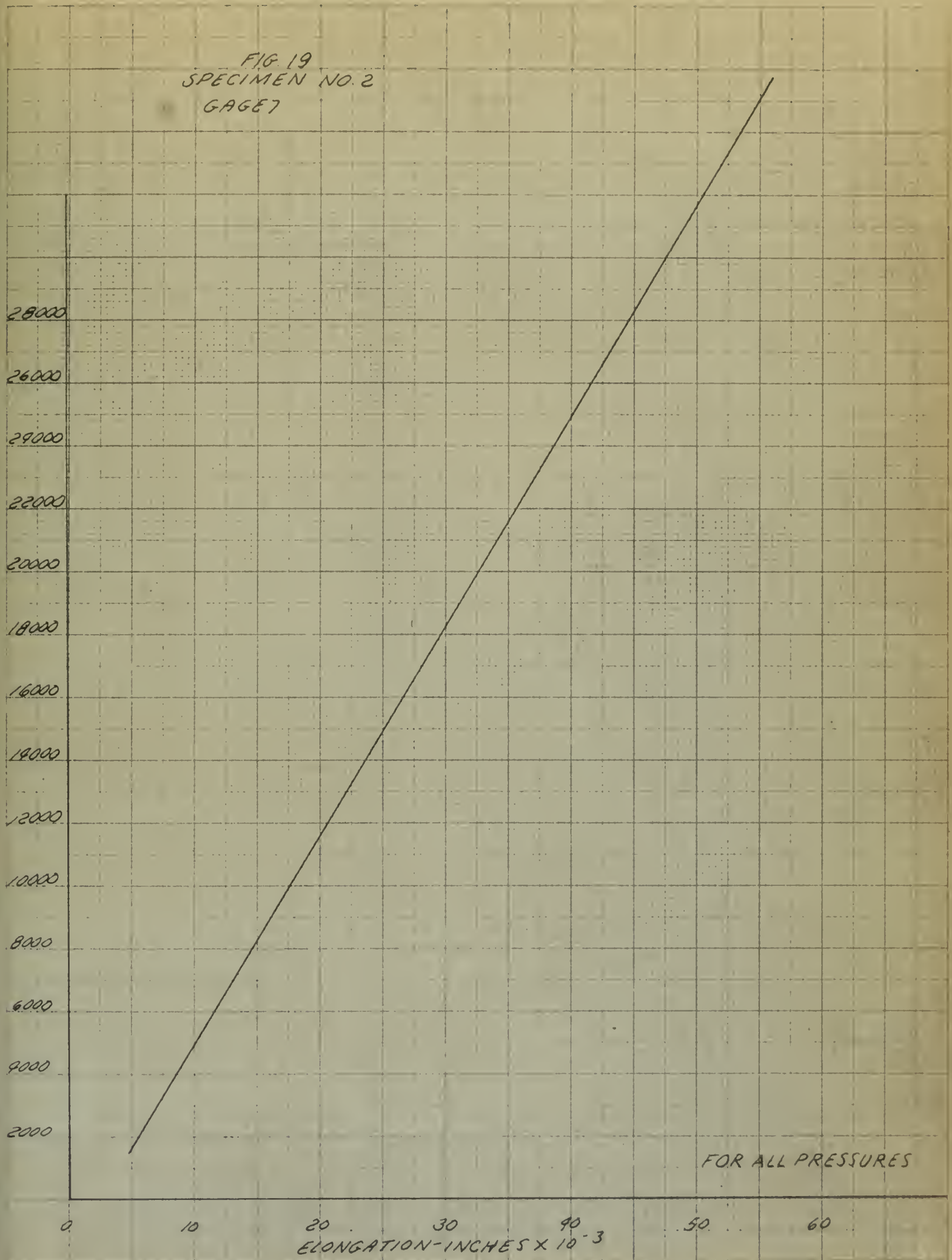

σ STRESS - PSI

FIG 20
SPECIMEN NO. 2
GAGE 8

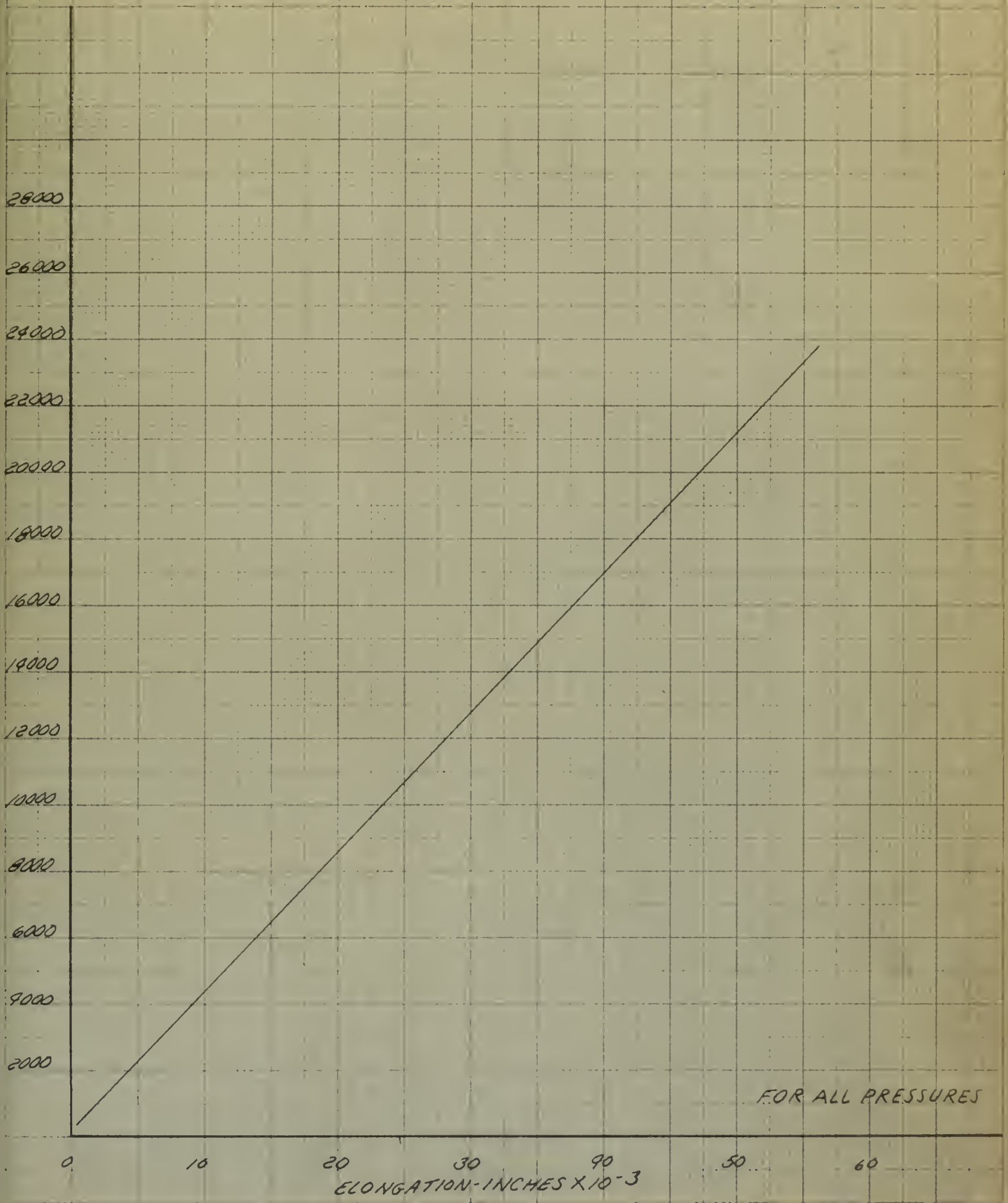

FIG. 21
SPECIMEN NO. 2
AVERAGE VALUES
FOR ELEMENT IN
CENTER OF EXPANSION
JOINT

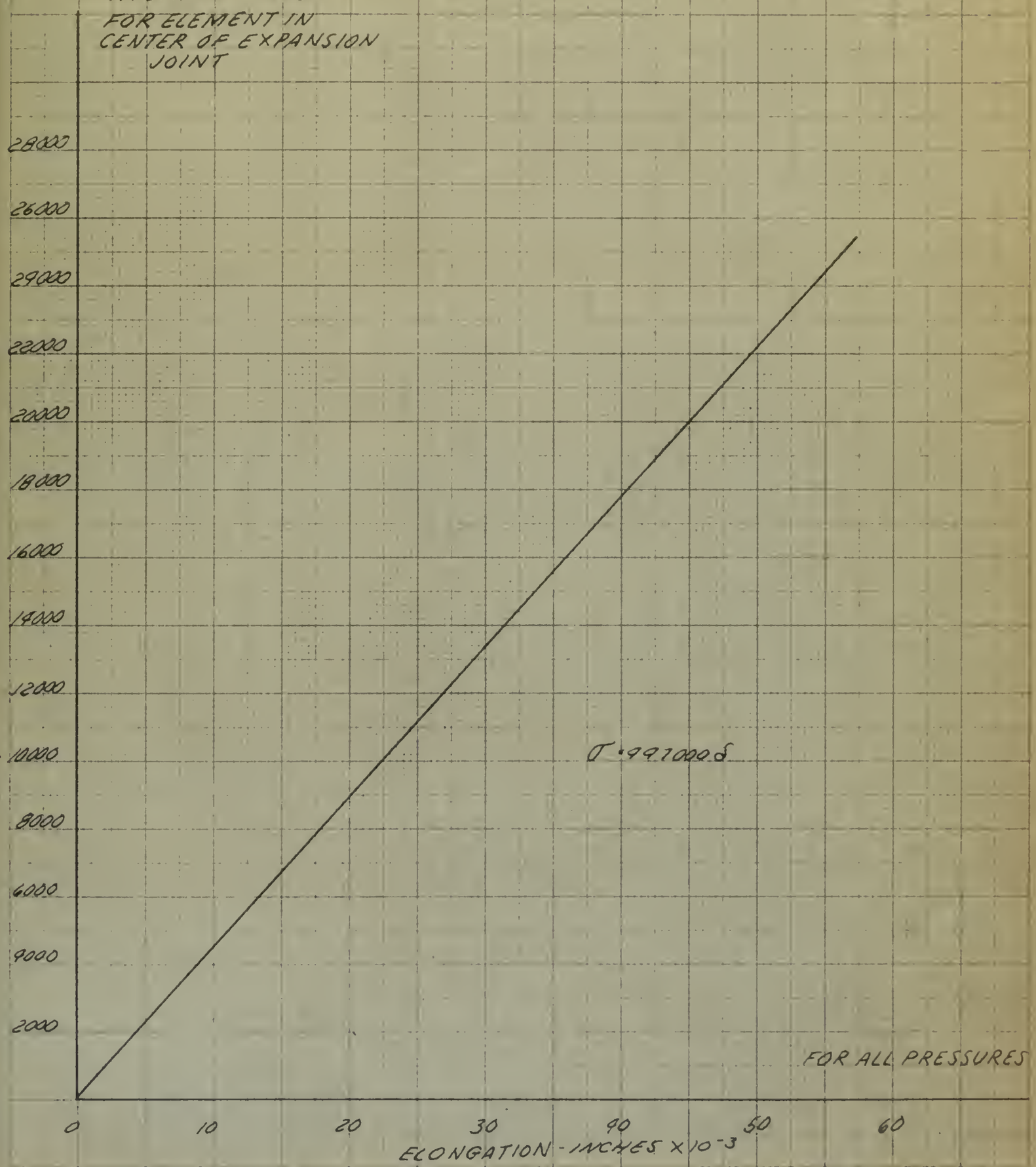

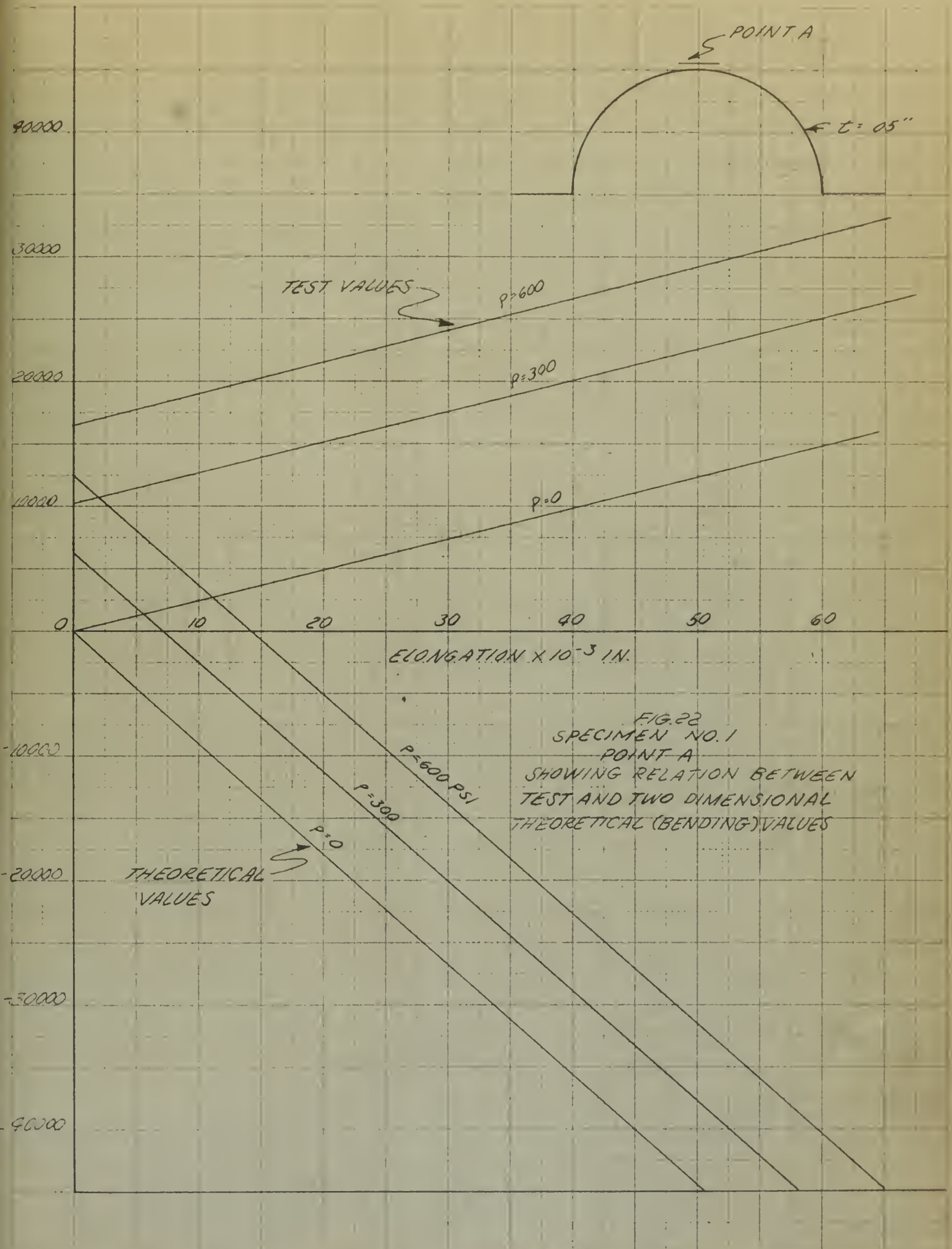

FIG. 22
SPECIMEN NO. 1
POINT A
SHOWING RELATION BETWEEN
TEST AND TWO DIMENSIONAL
THEORETICAL (BENDING) VALUES

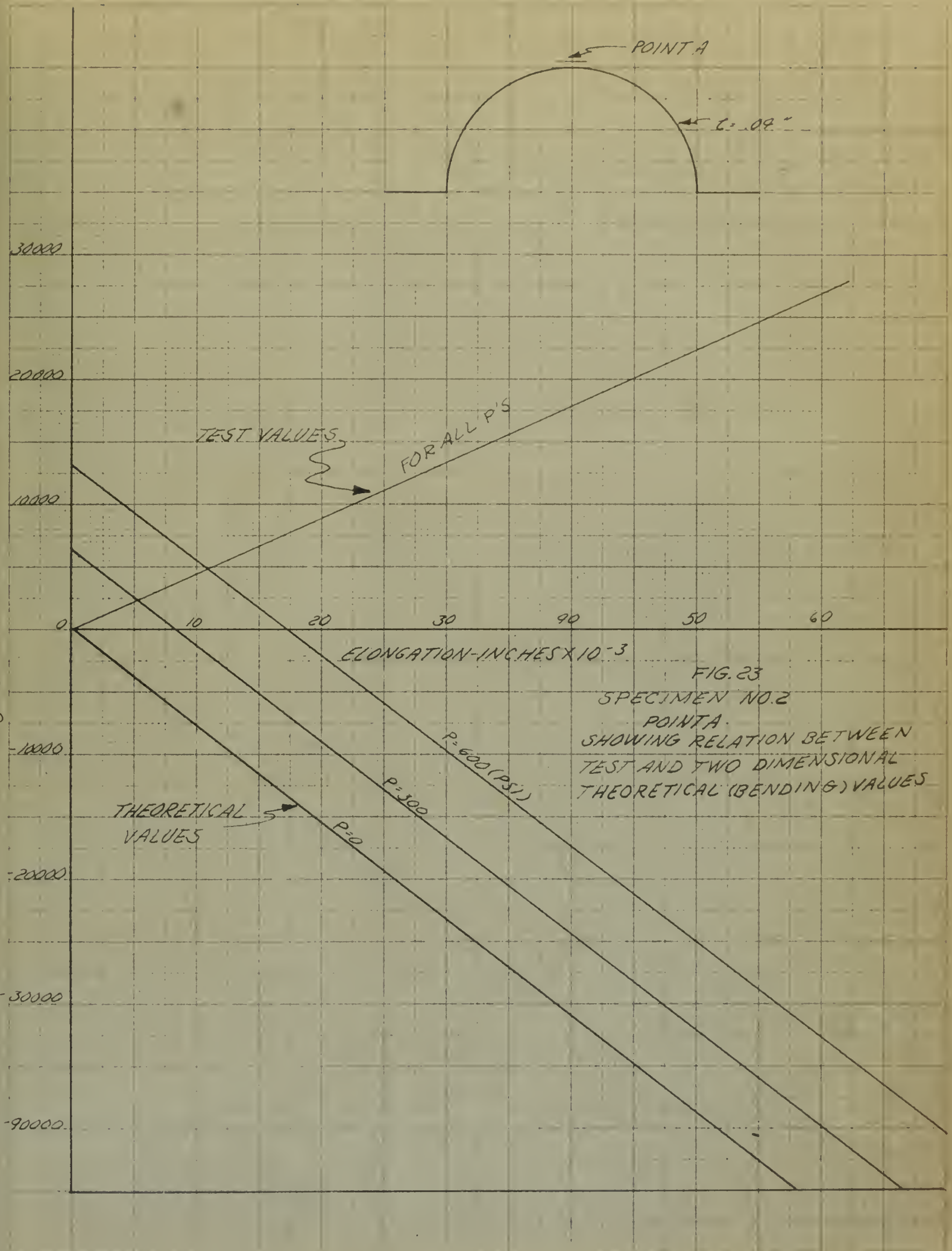

FIG. 23
SPECIMEN NO. 2
POINT A.
SHOWING RELATION BETWEEN
TEST AND TWO DIMENSIONAL
THEORETICAL (BENDING) VALUES

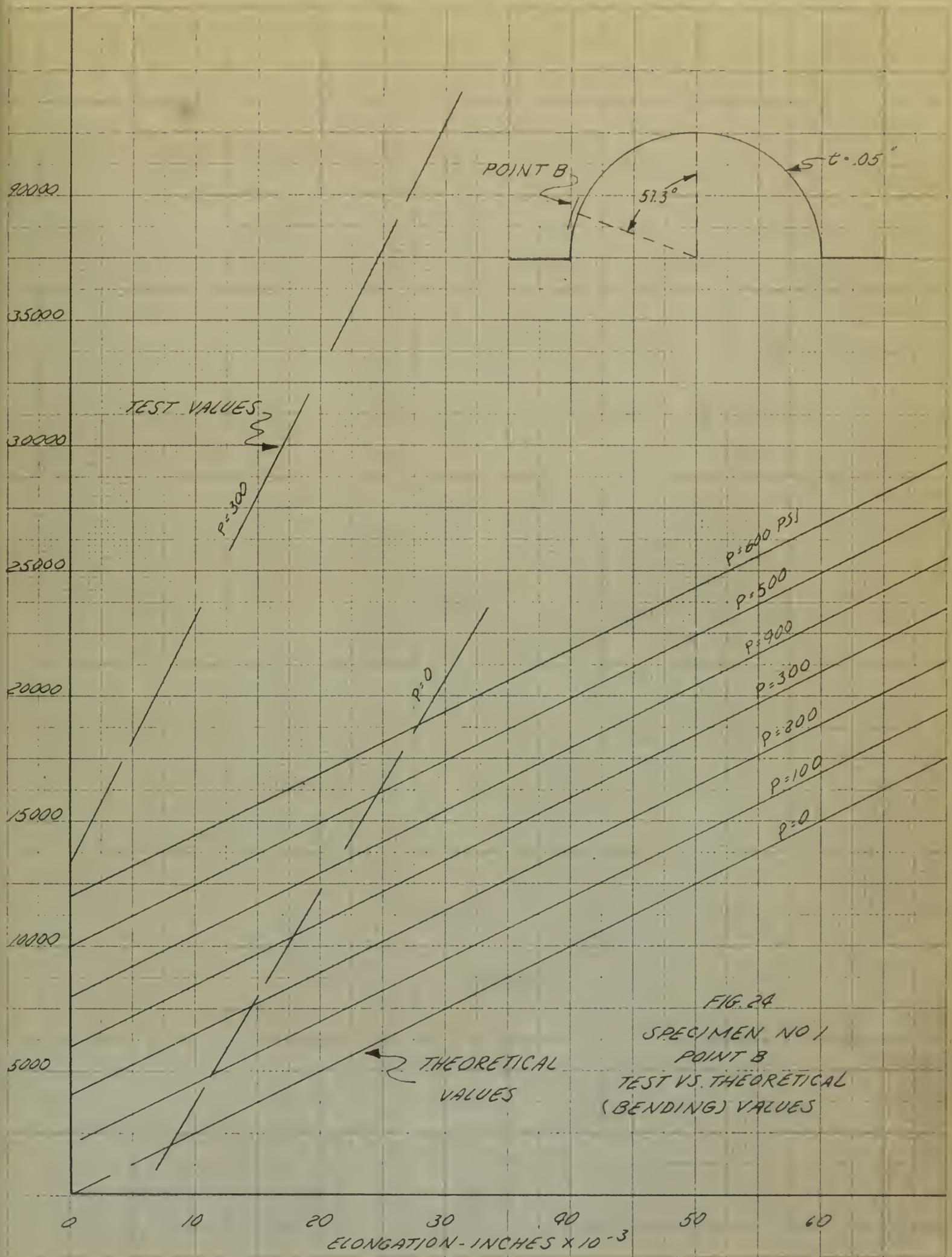

FIG. 24
SPECIMEN NO 1
POINT B
TEST VS. THEORETICAL
(BENDING) VALUES

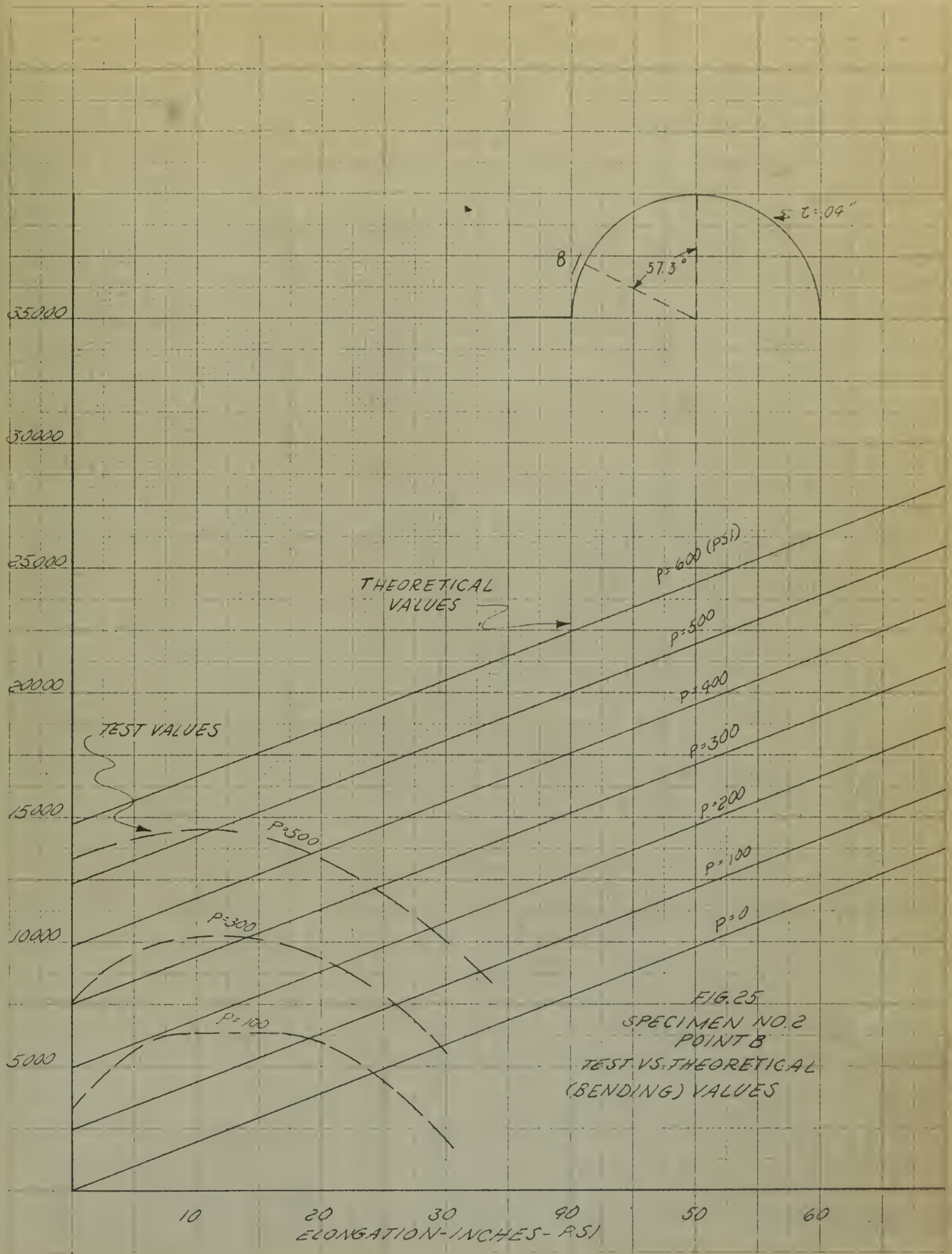

FIG. 25
SPECIMEN NO. 2
POINT B
TEST VS. THEORETICAL
(BENDING) VALUES

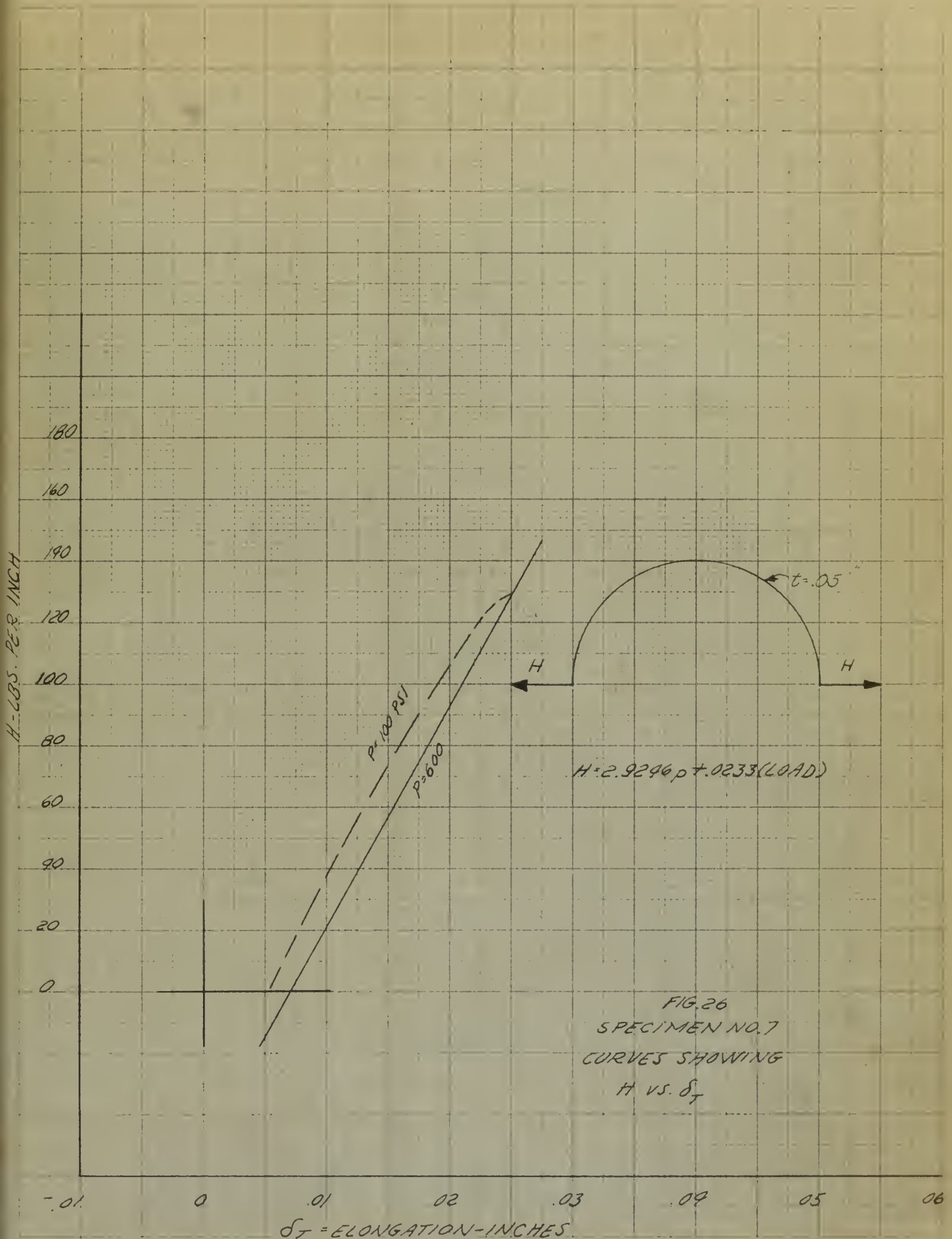

FIG. 26
SPECIMEN NO. 7
CURVES SHOWING
H VS. δ_T

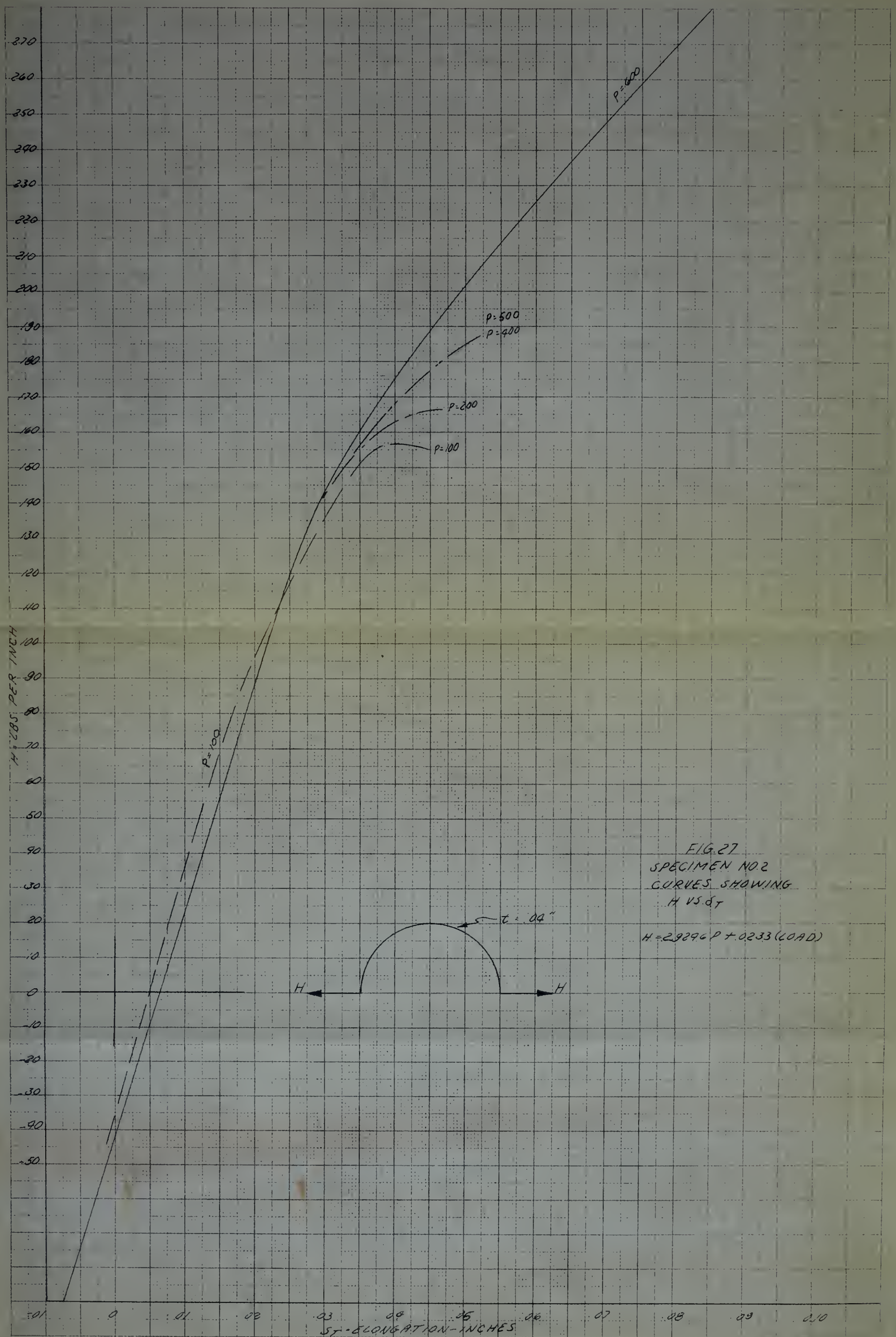

FIG. 27
SPECIMEN NO. 2
CURVES SHOWING
H VS. δ_T

$H = 2.9296\,P + .0233$ (LOAD)

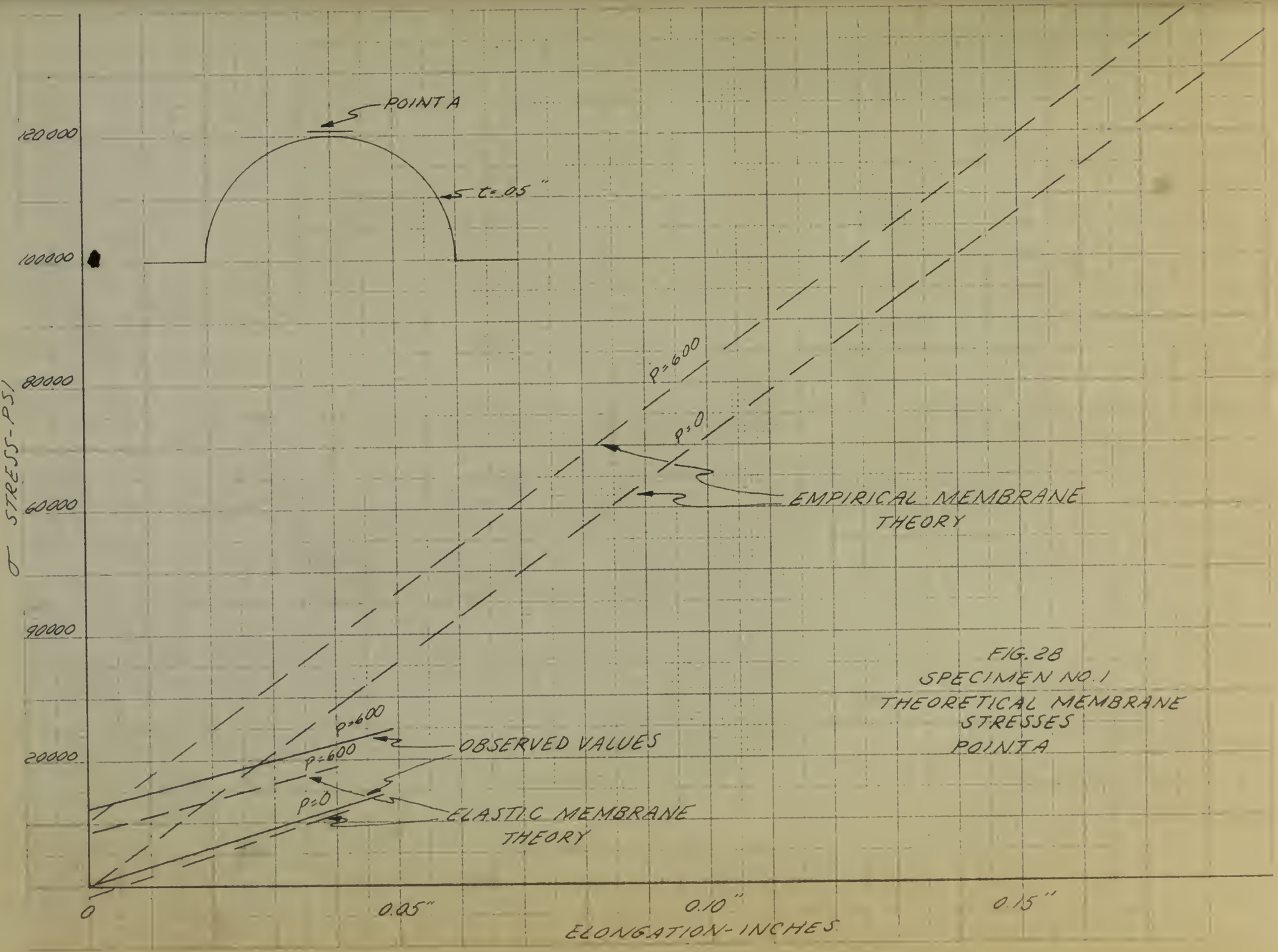

FIG. 28
SPECIMEN NO. 1
THEORETICAL MEMBRANE STRESSES
POINT A

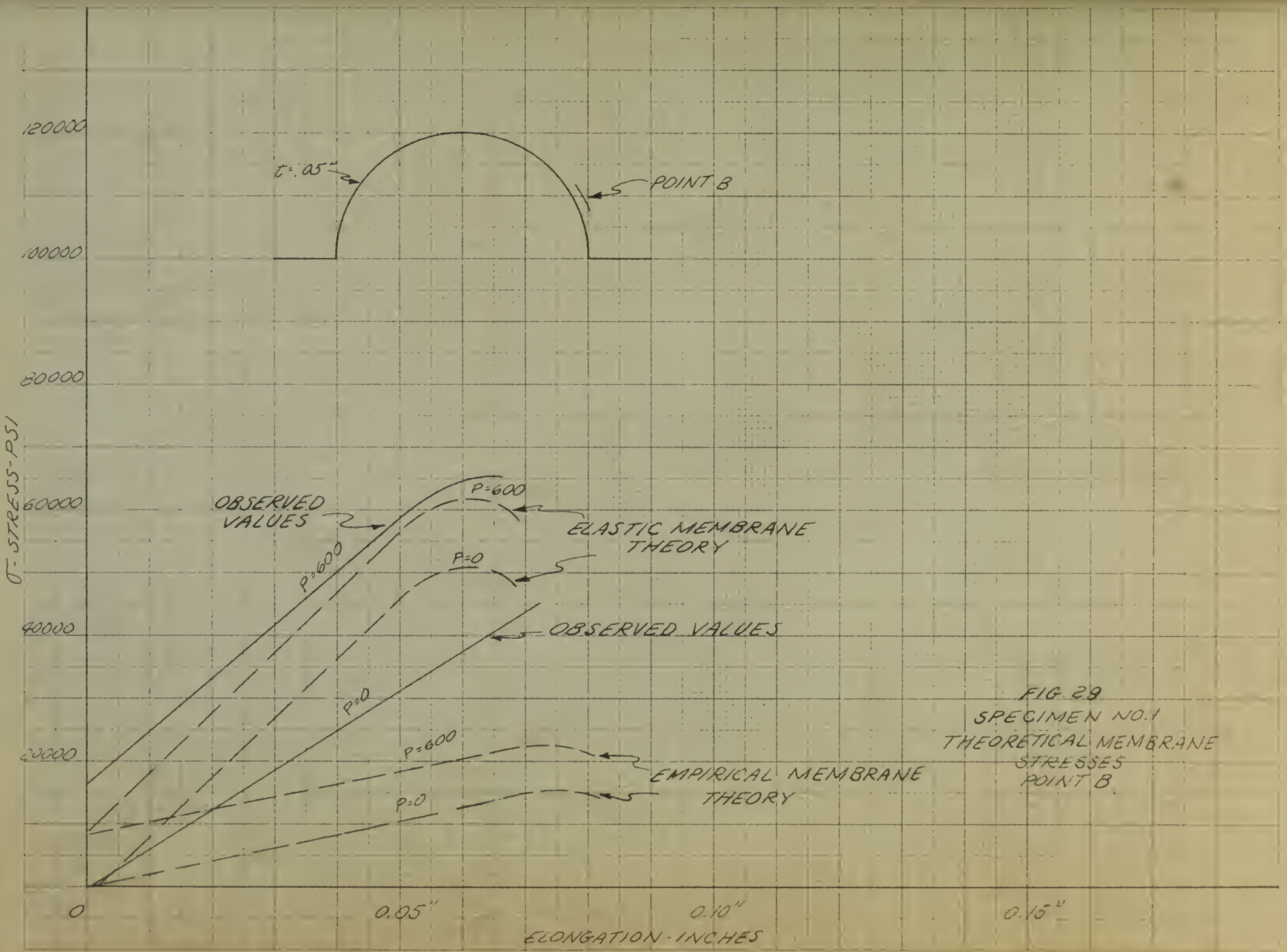

FIG. 28
SPECIMEN NO. 1
THEORETICAL MEMBRANE STRESSES
POINT B.

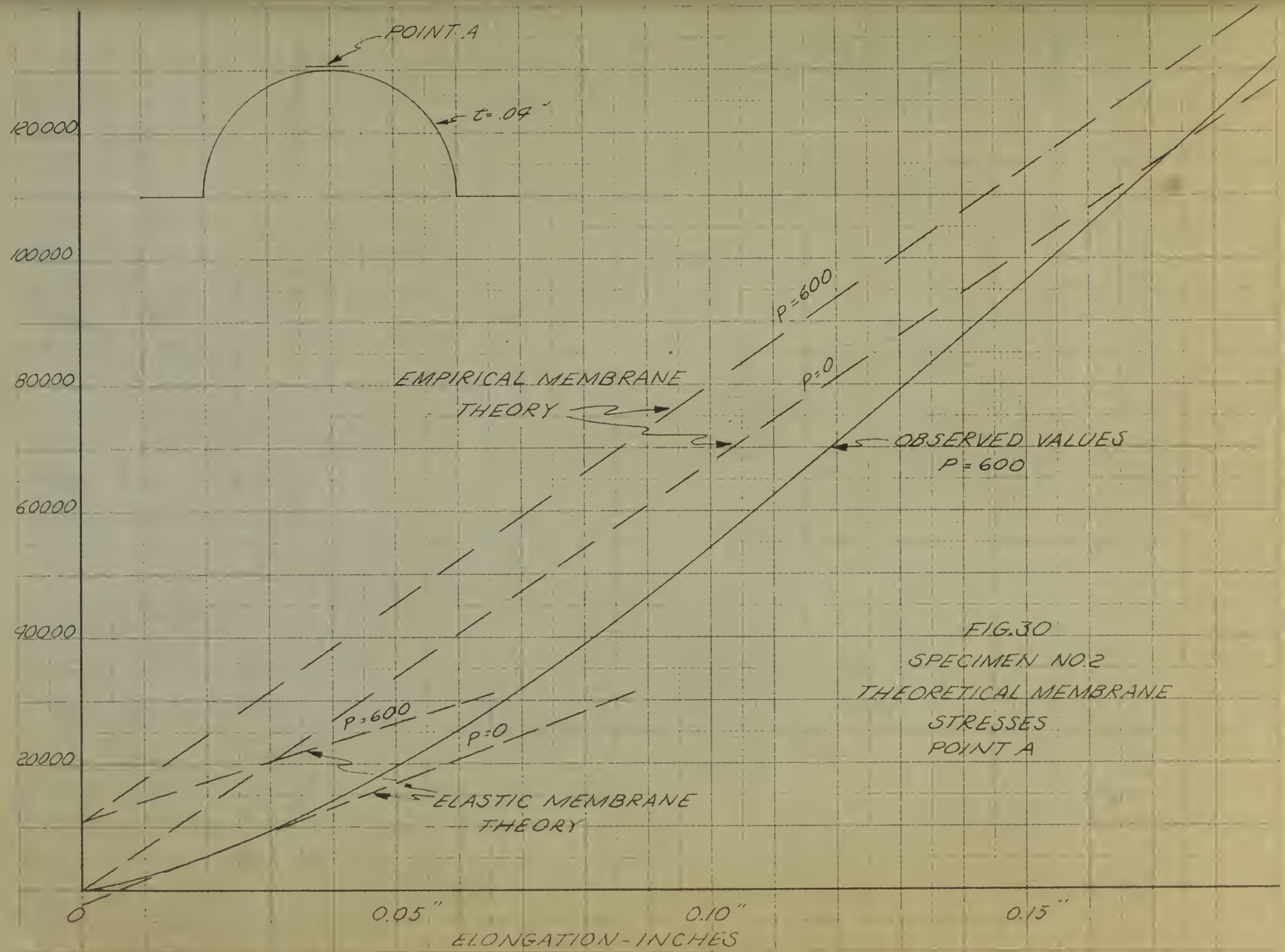

FIG.30
SPECIMEN NO.2
THEORETICAL MEMBRANE
STRESSES
POINT A

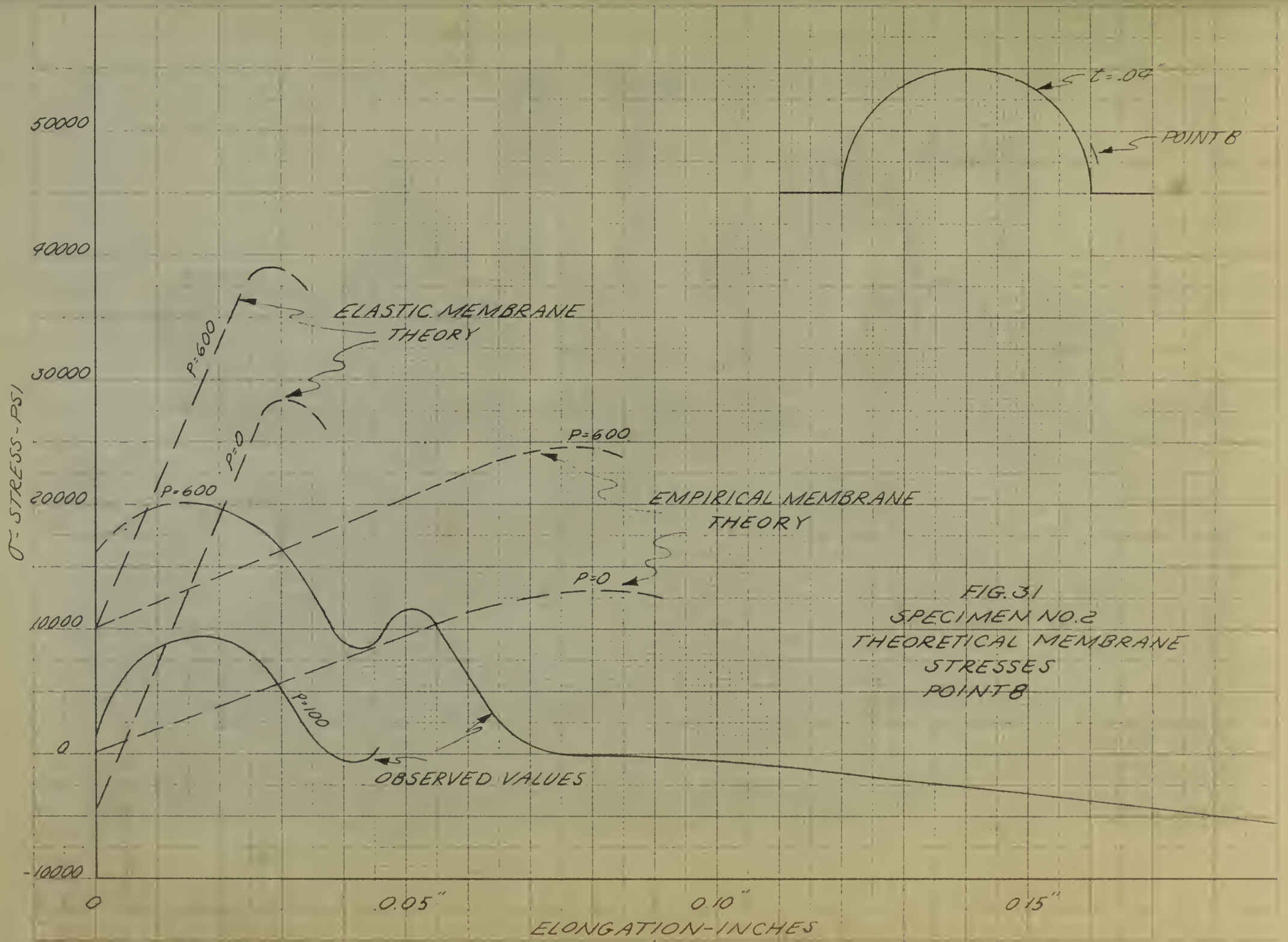

FIG. 31
SPECIMEN NO. 2
THEORETICAL MEMBRANE
STRESSES
POINT B

PHOTOGRAPH NO. I

PHOTOGRAPH NO. 11

U.S.N.A.P.
89

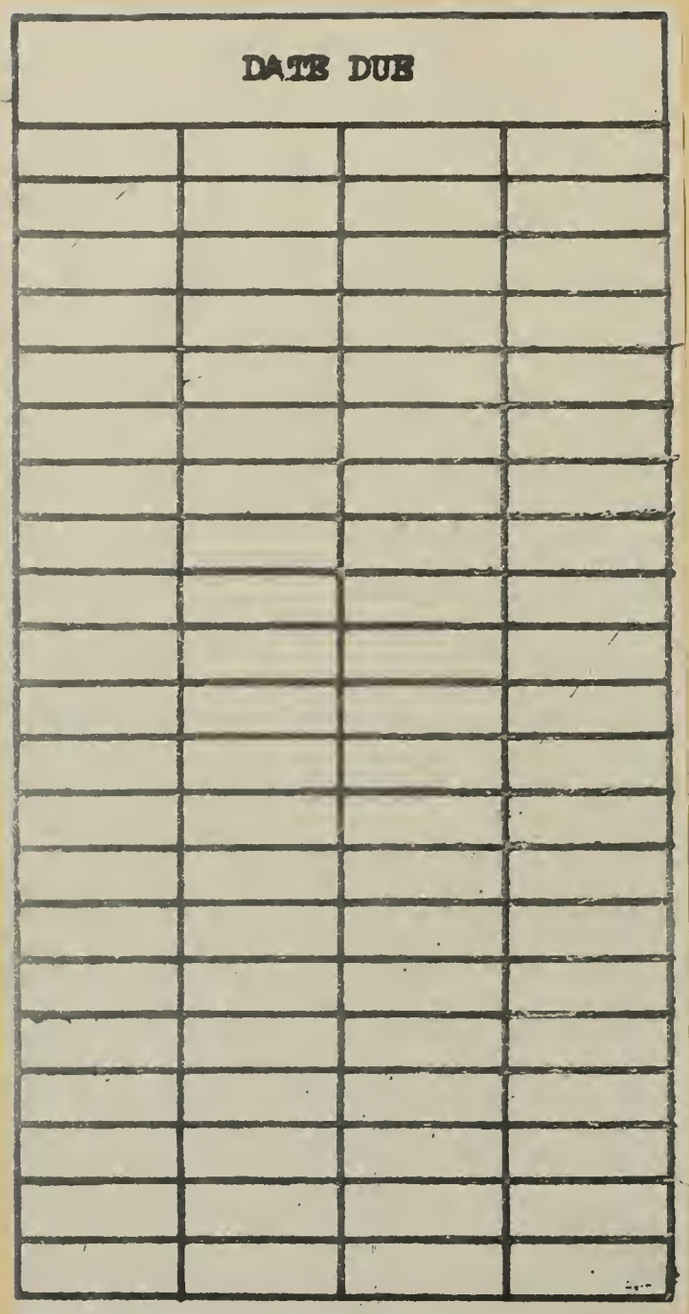
DATE DUE

Thesis
K58 Kleiss 15463
Some studies of ex-
pansion rings in rocket
motors.

Thesis 15463
K58 Kleiss
Some studies of ex-
pansion rings in rocket
motors.

thesK58
Some studies of expansion rings in rocke
3 2768 002 10625 4
DUDLEY KNOX LIBRARY